Organometallics **2008,** *27,* 857–871

Metallacumulenylidene Complexes in the Cycloheptatrienyl Molybdenum Series $[\mathrm{Mo}\{(\mathrm{C})_n{=}\mathrm{CR_2}\}\mathrm{L_2}(\eta\text{-}\mathrm{C_7H_7})]^+$ ($n = 0-2$; $\mathrm{L_2}$ = P-Donor Ligand). X-ray Crystal Structures of $[\mathrm{Mo}\{\mathrm{C{=}C(H)Ph}\}\{\mathrm{P(OMe)_3}\}_2(\eta\text{-}\mathrm{C_7H_7})][\mathrm{BF_4}]$ and $[\mathrm{Mo(C{=}C{=}CPh_2)(dppe)}(\eta\text{-}\mathrm{C_7H_7})][\mathrm{PF_6}]$ and DFT Investigation of Cumulenylidene Ligand Orientations

Richard W. Grime, Madeleine Helliwell, Zaffar I. Hussain, Hannah N. Lancashire,
Christopher R. Mason, Joseph J. W. McDouall, Christopher M. Mydlowski, and
Mark W. Whiteley*

School of Chemistry, University of Manchester, Manchester M13 9PL, U.K.

Received September 14, 2007

A series of metallacumulenylidene complexes of the cycloheptatrienyl molybdenum auxiliary $[\mathrm{Mo}\{(\mathrm{C})_n{=}\mathrm{CR_2}\}\mathrm{L_2}(\eta\text{-}\mathrm{C_7H_7})]^+$ ($n = 0-2$; $\mathrm{L_2}$ = P-donor ligand) have been synthesized by reaction of $[\mathrm{MoXL_2}(\eta\text{-}\mathrm{C_7H_7})]$ (X = Br, $\mathrm{L_2} = \mathrm{Ph_2PCH_2CH_2PPh_2}$ (dppe); X = I, $\mathrm{L_2} = 2\mathrm{P(OMe)_3}$) or $[\mathrm{Mo(OCMe_2)L_2}(\eta\text{-}\mathrm{C_7H_7})]^+$ ($\mathrm{L_2}$ = dppe, $\mathrm{Ph_2PCH_2PPh_2}$ (dppm)) with the terminal alkynes $\mathrm{HC{\equiv}CR}$; use of $[\mathrm{MoBr(dppe)}(\eta\text{-}\mathrm{C_7H_7})]$ as a precursor is facilitated by an improved, one-step synthesis from $[\mathrm{MoBr(CO)_2}(\eta\text{-}\mathrm{C_7H_7})]$. Syntheses of the 2-oxacyclocarbene complexes $[\mathrm{Mo}(\overline{\mathrm{CCH_2CH_2(CH_2)_{\mathit{x}}O}})\mathrm{L_2}(\eta\text{-}\mathrm{C_7H_7})]^+$ ($x = 1$, $\mathrm{L_2}$ = dppm (**1**), dppe (**2**); $x = 2$, $\mathrm{L_2}$ = dppm (**3**), $\mathrm{L_2}$ = dppe (**4**)), the vinylidenes $[\mathrm{Mo}\{\mathrm{C{=}C(H)(CH_2)_2CH_2OH}\}(\mathrm{dppe})(\eta\text{-}\mathrm{C_7H_7})][\mathrm{PF_6}]$ (**5**), $[\mathrm{Mo}\{\mathrm{C{=}C(H)(CH_2)_{\mathit{x}}Ph}\}(\mathrm{dppe})(\eta\text{-}\mathrm{C_7H_7})]^+$ ($x = 2$ (**6**), 1 (**7**)), and $[\mathrm{Mo}\{\mathrm{C{=}C(H)Ph}\}\{\mathrm{P(OMe)_3}\}_2(\eta\text{-}\mathrm{C_7H_7})]^+$ (**8**), and the first examples of monometallic molybdenum allenylidene complexes, $[\mathrm{Mo(C{=}C{=}CRPh)(dppe)}(\eta\text{-}\mathrm{C_7H_7})]^+$ (R = Ph (**9**), Me (**10**)) are reported. X-ray structural studies on complexes **8** and **9** have determined Mo−C$_\alpha$ distances as follows: **8**, 1.929(3) Å; **9**, 1.994(3) Å. In **8**, the vinylidene ligand substituents lie in the pseudo mirror plane of the $\mathrm{MoL_2}(\eta\text{-}\mathrm{C_7H_7})$ auxiliary (vertical orientation) with the phenyl group located syn to the cycloheptatrienyl ring, whereas the allenylidene ligand substituents of **9** are perpendicular to the pseudo mirror plane (horizontal orientation). This series of atypical orientations of cumulenylidene ligand substituents, imposed by the cycloheptatrienyl molybdenum auxiliary, has been investigated further by variable-temperature NMR spectroscopy and quantum-chemical theoretical calculations. A DFT analysis of the complexes $[\mathrm{Mo(C{=}CH_2)(dppe)}(\eta\text{-}\mathrm{C_7H_7})]^+$ (**11**), $[\mathrm{Ru(C{=}CH_2)(dppe)Cp}]^+$ (**12**), and $[\mathrm{Mo(C{=}C{=}CMePh)(dppe)}(\eta\text{-}\mathrm{C_7H_7})]^+$ (**10**) concurs with experimentally determined cumulenylidene ligand orientations. A separate analysis of the fragments $[\mathrm{Mo(dppe)}(\eta\text{-}\mathrm{C_7H_7})]^+$ and $[\mathrm{Ru(dppe)Cp}]^+$ reveals that the HOMO of the $[\mathrm{Mo(dppe)}(\eta\text{-}\mathrm{C_7H_7})]^+$ fragment includes a significant contribution from the metal d_{z^2} orbital, whereas the HOMO of the $[\mathrm{Ru(dppe)Cp}]^+$ fragment is based on a metal d_{xy} orbital, orthogonal to the HOMO of the $[\mathrm{Mo(dppe)}(\eta\text{-}\mathrm{C_7H_7})]^+$ unit. In cumulenylidene complexes of the $\mathrm{Mo(dppe)}(\eta\text{-}\mathrm{C_7H_7})$ auxiliary, interactions between the d_{z^2}-based HOMO of the metal fragment and the vacant LUMO of the cumulenylidene ligand dominate the control of ligand orientation and thus account for the observed structures.

Introduction

Complexes containing highly unsaturated carbon chain ligands, σ-bonded to a transition-metal center,[1–3] constitute a field of intense current activity in organometallic chemistry, with potential applications in the development of molecular devices[4] and the preparation of metallopolymers.[5] Two series of complexes, key to the development of this work, are the alkynyl and polyynyl systems $\mathrm{M{-}(C{\equiv}C)_{\mathit{n}}C{\equiv}CR}$[1] and the metallacumulenylidenes $\mathrm{M(C)_{\mathit{n}}{=}CR_2}$.[2,3,6] Although an extensive chemistry of the group 7 and 8 transition metals has evolved in this area, the use of group 6 metal supporting auxiliaries is less common. Thus, while the synthetic applications of group 6 metal carbene complexes are legion,[7,8] examples of vinylidene derivatives are quite scarce[6,9–12] and higher homologues are restricted

---

* To whom correspondence should be addressed. Tel: 0161 275 4634. Fax: 0161 275 4598. E-mail: Mark.Whiteley@manchester.ac.uk.

(1) Bruce, M. I. *Chem. Rev.* **1998**, *98*, 2797.
(2) Bruce, M. I. *Coord. Chem. Rev.* **2004**, *248*, 1603.
(3) Low, P. J.; Bruce, M. I. *Adv. Organomet. Chem.* **2002**, *48*, 71.
(4) Long, N. J.; Williams, C. K. *Angew. Chem., Int. Ed.* **2003**, *42*, 2586.
(5) Manners, I. *Synthetic Metal-Containing Polymers*; Wiley-VCH: Weinheim, Germany, 2004; Chapter 5.
(6) Bruce, M. I. *Chem. Rev.* **1991**, *91*, 197.
(7) Barluenga, J. *Pure, Appl. Chem.* **1996**, *68*, 543.
(8) Gómez-Gallego, M.; Mancheño, M. J.; Sierra, M. A. *Acc. Chem. Res.* **2005**, *38*, 44.
(9) Selegue, J. P. *Coord. Chem. Rev.* **2004**, *248*, 1543.
(10) Ipaktschi, J.; Mohsseni-Ala, J.; Uhlig, S. *Eur. J. Inorg. Chem.* **2003**, 4313.
(11) Yang, J.-Y.; Huang, S.-L.; Lin, Y.-C.; Liu, Y.-H.; Wang, Y. *Organometallics* **2000**, *19*, 269.
(12) Bartlett, I. M.; Connelly, N. G.; Martin, A. J.; Orpen, A. G.; Paget, T. J.; Rieger, A. L.; Rieger, P. H. *J. Chem. Soc., Dalton Trans.* **1999**, 691.

10.1021/om700920t CCC: $40.75

essentially to complexes of the type $[M\{(C)_n{=}CR_2\}(CO)_5]$ (M = Cr, W).[2,3,13]

Our interest in this field has focused on the application of the $Mo(\eta\text{-}C_7H_7)$ (cycloheptatrienyl molybdenum) auxiliary as the supporting group in metal alkynyl, polyynyl, and cumulenylidene complexes, and we have previously described examples of alkynyl,[14] butadiynyl,[15] and vinylidene[16] complexes of the electron-rich system $Mo(dppe)(\eta\text{-}C_7H_7)$ (dppe = $Ph_2PCH_2CH_2PPh_2$). The enhanced stability of the vinylidene configuration over the isomeric alkyne form, imposed by the formally d^6, electron-rich, cycloheptatrienyl molybdenum center is in contrast to the relative stabilities of these ligand types in complexes with d^4 cyclopentadienyl molybdenum/tungsten centers $M(CO)L_2Cp$ (M = Mo, W; $L_2 = 2P(OMe)_3$,[17] dppe,[11] etc.), and this renders the $Mo(dppe)(\eta\text{-}C_7H_7)$ auxiliary particularly suitable for the convenient synthesis and isolation of stable complexes of the vinylidene ligand and its higher homologues. Furthermore, our investigations have shown that the $Mo(dppe)(\eta\text{-}C_7H_7)$ auxiliary brings a series of useful and, in some cases, unique properties to this chemistry, including low redox potentials for one-electron oxidation processes,[15,18] highly resolved EPR spectra of 17-electron radical cations,[19] steric protection of reactive sites on the carbon chain ligand,[20,21] and a novel orientational preference for cumulenylidene ligand R substituents.[16] In this paper we report on the synthesis and structures of an extended series of cumulenylidene complexes $[Mo\{(C)_n{=}CR_2\}L_2(\eta\text{-}C_7H_7)]^+$ (n = 0 (carbene), 1, (vinylidene), 2 (allenylidene); L_2 = P-donor ligand) and explore in depth the origin of the unusual structural orientation of cumulenylidene ligands coordinated to the $Mo(\eta\text{-}C_7H_7)$ auxiliary; part of the work on carbene complexes has been communicated previously.[21]

Results and Discussion

Synthetic Studies. An extensive chemistry of carbene, vinylidene, and allenylidene complexes of d^6 group 8 metal auxiliaries $ML_2(\eta\text{-}C_xH_y)$ (M = Fe, L_2 = dppe, C_xH_y = Cp,[22] Cp*;[23,24] M = Ru, L_2 = $2PR_3$, dppe, C_xH_y = Cp,[25–28] indenyl (C_9H_7)[29–31]) has been developed on the basis of the reaction of metal halide precursor complexes $[MXL_2(\eta\text{-}C_xH_y)]$ with terminal alkynes $HC{\equiv}CR$ in methanol in the presence of a halide acceptor such as $NH_4[PF_6]$ or $K[PF_6]$. The method depends upon ionization of the halide ligand and subsequent addition of the alkyne to the metal center; the lability of the halide to dissociation exhibits a strong dependence upon the identity of the $ML_2(\eta\text{-}C_xH_y)$ auxiliary,[32] with [FeCl(dppe)Cp*] being reactive at ambient temperature[24] while $[RuCl(PPh_3)_2Cp]$ generally requires reflux conditions for the reaction to proceed.[33] Alternative synthetic protocols based on reactions of $HC{\equiv}CR$ with the preformed solvato complexes $[M(sol)L_2(\eta\text{-}C_xH_y)]^+$ have also been reported,[34] but these are less frequently employed due to the ready availability of the halide complexes and the convenience of their subsequent reactions with alkynes. As we have demonstrated previously, the structurally analogous d^6 cycloheptatrienyl molybdenum auxiliary $MoL_2(\eta\text{-}C_7H_7)$ (L_2 = dppm, dppe) also promotes the rearrangement of terminal alkynes to a series of vinylidene complexes.[14,16] However, in contrast to the related iron and ruthenium systems, the halide precursors $[MoXL_2(\eta\text{-}C_7H_7)]$ have not been readily available and therefore the majority of our previous work has been derived from reactions of alkynes with $[Mo(sol)L_2(\eta\text{-}C_7H_7)]^+$ (sol = acetone), generated in situ from the sandwich complex $[Mo(\eta\text{-}C_6H_5Me)(\eta\text{-}C_7H_7)][PF_6]$ and L_2 in acetone. Although this synthetic protocol continues to be useful in the current work, the development of an improved route to the halide complex $[MoBr(dppe)(\eta\text{-}C_7H_7)]$ now provides an alternative and more convenient procedure.

The direct reaction of $[MoX(CO)_2(\eta\text{-}C_7H_7)]$ (X = halide) with dppe in refluxing toluene[35] proceeds via the ring-slipped complex $[MoX(CO)_2(dppe)(\eta^3\text{-}C_7H_7)]$[36] to give a mixture of $[Mo(CO)(dppe)(\eta\text{-}C_7H_7)]X$ and $[MoX(dppe)(\eta\text{-}C_7H_7)]$, but the former product is the major component of the reaction mixture and its poor solubility impedes further reaction. However, when dppe is added to a refluxing toluene solution of $[MoBr(CO)_2(\eta\text{-}C_7H_7)]$ in two $^1/_2$ equiv quantities separated by a period of 1 h, the yield of the required halide complex is significantly enhanced and it is obtained as $[MoBr(dppe)(\eta\text{-}C_7H_7)]\cdot 0.5CH_2Cl_2$ following purification by chromatography on alumina and recrystallization from CH_2Cl_2/hexane. This development opens up the cycloheptatrienyl molybdenum system to a much wider reaction chemistry with terminal alkynes and has been critical to obtaining an extended range of metallacumulenylidenes $[Mo\{(C)_n{=}CR_2\}L_2(\eta\text{-}C_7H_7)]^+$ (n = 0–2; L_2 = P-donor ligand).

The reactions of $[Mo(OCMe_2)L_2(\eta\text{-}C_7H_7)]^+$ (L_2 = dppe, dppm) and $[MoXL_2(\eta\text{-}C_7H_7)]$ (X = Br, L_2 = dppe; X = I, L_2 = $2P(OMe)_3$[37]) with the terminal alkynes $HC{\equiv}C(CH_2)_xCH_2OH$, $HC{\equiv}C(CH_2)_xPh$, and $HC{\equiv}CCRPh(OH)$ have been employed

---

(13) Fischer, H.; Szesni, N. *Coord. Chem. Rev.* **2004**, *248*, 1659.

(14) Adams, J. S.; Bitcon, C.; Brown, J. R.; Collison, D.; Cunningham, M.; Whiteley, M. W. *J. Chem. Soc., Dalton Trans.* **1987**, 3049.

(15) Lancashire, H. N.; Ahmed, R; Hague, T. L.; Helliwell, M.; Hopgood, G. A.; Sharp, L.; Whiteley, M. W. *J. Organomet. Chem.* **2006**, *691*, 3617.

(16) Beddoes, R. L.; Bitcon, C.; Grime, R. W.; Ricalton, A.; Whiteley, M. W. *J. Chem. Soc., Dalton Trans.* **1995**, 2873.

(17) Nicklas, P. N.; Selegue, J. P.; Young, B. A. *Organometallics* **1988**, *7*, 2248.

(18) Bitcon, C.; Whiteley, M. W. *J. Organomet. Chem.* **1987**, *336*, 385.

(19) Aston, G. M.; Badriya, S.; Farley, R. D.; Grime, R. W.; Ledger, S. J.; Mabbs, F. E.; McInnes, E. J. L.; Morris, H. W.; Ricalton, A.; Rowlands, C. C.; Wagner, K.; Whiteley, M. W. *J. Chem. Soc., Dalton Trans.* **1999**, 4379.

(20) Fitzgerald, E. C.; Grime, R. W.; Knight, H. C.; Helliwell, M.; Raftery, J.; Whiteley, M. W. *J. Organomet. Chem.* **2006**, *691*, 1879.

(21) Beddoes, R. L.; Grime, R. W.; Hussain, Z. I.; Whiteley, M. W. *J. Chem. Soc., Dalton Trans.* **1996**, 3893.

(22) Consiglio, G.; Bangerter, F.; Darpin, C.; Morandini, F.; Lucchini, V. *Organometallics* **1984**, *3*, 1446.

(23) Connelly, N. G.; Gamasa, M. P.; Gimeno, G.; Lapinte, C.; Lastra, E.; Maher, J. P.; Le Narvor, N.; Rieger, A. L.; Rieger, P. H. *J. Chem. Soc., Dalton Trans.* **1993**, 2575.

(24) Argouarch, G.; Thominot, P.; Paul, F.; Toupet, L.; Lapinte, C. *C. R. Chim.* **2003**, *6*, 209.

(25) Bruce, M. I.; Swincer, G. A.; Thomson, B. J.; Wallis, R. C. *Aust. J. Chem.* **1980**, *33*, 2605.

(26) Bruce, M. I.; Wallis, R. C. *Aust. J. Chem.* **1979**, *32*, 1471.

(27) Beddoes, R. L.; Grime, R. W.; Hussain, Z. I.; Whiteley, M. W. *J. Organomet. Chem.* **1996**, *526*, 371.

(28) Selegue, J. P. *Organometallics* **1982**, *1*, 217.

(29) Gamasa, M. P.; Gimeno, J.; Martín-Vaca, B. M.; Isea, R.; Vegas, A. *J. Organomet. Chem.* **2002**, *651*, 22.

(30) Gamasa, M. P.; Gimeno, J.; Martín-Vaca, B. M.; Borge, J.; García-Granda, S; Pérez-Carreño, E. *Organometallics* **1994**, *13*, 4045.

(31) Cadierno, V.; Gamasa, M. P.; Gimeno, J.; González-Cueva, M.; Lastra, E.; Borge, J.; García-Granda, S.; Pérez-Carreño, E. *Organometallics* **1996**, *15*, 2137.

(32) Treichel, P. M.; Vincenti, P. J. *Inorg. Chem.* **1985**, *24*, 228.

(33) Bruce, M. I.; Ellis, B. G.; Gaudio, M.; Lapinte, C.; Melino, G.; Paul, F.; Skelton, B. W.; Smith, M. E.; Toupet, L.; White, A. H. *Dalton Trans.* **2004**, 1601.

(34) Schumann, H.; Admiraal, G.; Beurskens, P. T. *Z. Naturforsch.* **1992**, *47B*, 1125.

(35) Beall, T. W.; Houk, L. W. *Inorg. Chem.* **1973**, *12*, 1979.

(36) Beddoes, R. L.; Hussain, Z. I.; Roberts, A.; Barraclough, C. R.; Whiteley, M. W. *J. Chem. Soc., Dalton Trans.* **1996**, 3629.

(37) Bitcon, C.; Breeze, R.; Miller, P. F.; Whiteley, M. W. *J. Organomet. Chem.* **1989**, *364*, 181.

Scheme 1[a]

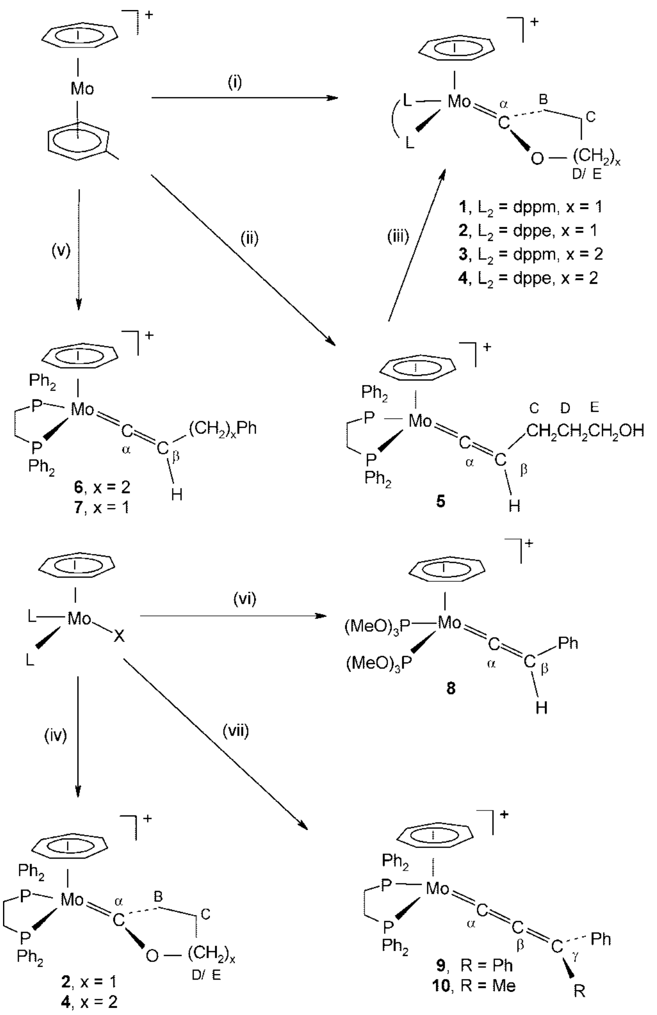

[a] Reagents and conditions: (i) dppe or dppm in acetone, reflux 18 h, then add $HC{\equiv}C(CH_2)_xOH$ ($x = 2, 3$) reflux 3 h, **1**–**3** only; (ii) dppe in acetone, reflux 18 h, then add $HC{\equiv}C(CH_2)_3OH$, reflux 30 min; (iii) LiCl, reflux in acetone, reflux 18 h (**5** to **4** only); (iv) X = Br, L_2 = dppe; $HC{\equiv}C(CH_2)_xOH/K[PF_6]$ methanol reflux, $x = 2$, 1.5 h; $x = 3$, 72 h; (v) dppe in acetone, reflux 18 h, then add $HC{\equiv}C(CH_2)_xPh$ (x = 1, 2), reflux 3 h; (vi) X = I, L_2 = 2 $P(OMe)_3$; $HC{\equiv}CPh/K[PF_6]$ stir in methanol, 20 °C, 3 h; (vii) X = Br, L_2 = dppe; $HC{\equiv}CCRPh(OH)/K[PF_6]$ methanol reflux, R = Ph, 12 h; R = Me, 2 h.

in the synthesis of a series of oxacyclocarbene (**1**- **4**), vinylidene (**5**–**8**), and allenylidene (**9**, **10**) complexes. The substance of the synthetic work is summarized in Scheme 1; clearly the group 6 cycloheptatrienyl molybdenum center is able to support a range of metallacumulenylidenes in a directly analogous manner to the widely reported group 8 Cp, Cp*, and indenyl systems.

The 2-oxacyclopentylidenes $[\mathrm{Mo}(\overline{\mathrm{CCH_2CH_2CH_2O}})\mathrm{L_2}(\eta\text{-}\mathrm{C_7H_7})][\mathrm{PF_6}]$ (L_2 = dppm (**1**), dppe (**2**)) and the 2-oxacyclohexylidene $[\mathrm{Mo}(\overline{\mathrm{CCH_2(CH_2)_2CH_2O}})(\mathrm{dppm})(\eta\text{-}\mathrm{C_7H_7})][\mathrm{PF_6}]$ (**3**) were obtained by treatment of the appropriate precursor, $[\mathrm{MoBr(dppe)}(\eta\text{-}\mathrm{C_7H_7})]$ or $[\mathrm{Mo(OCMe_2)L_2}(\eta\text{-}\mathrm{C_7H_7})]^+$, with 3-butyn-1-ol or 4-pentyn-1-ol, respectively, under reflux in methanol or acetone. In contrast, the reaction of $[\mathrm{Mo(OCMe_2)(dppe)}(\eta\text{-}\mathrm{C_7H_7})]^+$ with 4-pentyn-1-ol in refluxing acetone selectively formed the hydroxypropylvinylidene complex $[\mathrm{Mo\{C{=}C(H)(CH_2)_2CH_2OH\}(dppe)}(\eta\text{-}\mathrm{C_7H_7})][\mathrm{PF_6}]$ (**5**), the identity of which was suggested by infrared (ν(C=C) 1614 cm^{-1}) and $^{13}C\{^1H\}$ NMR ($\delta(C_\alpha)$ 369.5 ppm) data (see Table 1) and subsequently confirmed by an X-ray crystal structure.[21] Only after prolonged reflux in methanol or acetone did the intermediate **5** convert to the 2-oxacyclohexylidene $[\mathrm{Mo}(\overline{\mathrm{CCH_2(CH_2)_2CH_2O}})(\mathrm{dppe})(\eta\text{-}\mathrm{C_7H_7})][\mathrm{PF_6}]$ (**4**). This observation highlights the considerable steric protection afforded to C_α by the $\mathrm{Mo(dppe)}(\eta\text{-}\mathrm{C_7H_7})$ auxiliary, a property not so evident for the analogous ruthenium systems $\mathrm{RuL_2}(\eta\text{-}\mathrm{C}_x\mathrm{H}_y)$, for which only longer chain hydroxybutylvinylidene derivatives $[\mathrm{Ru\{C{=}C(H)(CH_2)_3CH_2OH\}L_2}(\eta\text{-}\mathrm{C_9H_7})]^+$ are isolable.[29] Consistent with this study, the previously reported vinylidene complexes $[\mathrm{Mo\{C{=}C(H)R\}(dppe)}(\eta\text{-}\mathrm{C_7H_7})]^+$, (R = H, Ph)[16] are unreactive toward formation of the alkoxycarbenes $[\mathrm{Mo\{C(OMe)CH_2R\}(dppe)}(\eta\text{-}\mathrm{C_7H_7})]^+$ in refluxing methanol; cyclization of ω-alkyn-1-ols is therefore currently the only route to carbene derivatives of the cycloheptatrienyl molybdenum system.

The two new vinylidene derivatives $[\mathrm{Mo\{C{=}C(H)R\}(dppe)}(\eta\text{-}\mathrm{C_7H_7})]^+$ (R = CH_2CH_2Ph (**6**), CH_2Ph (**7**)) have been obtained by reaction of $[\mathrm{Mo(OCMe_2)(dppe)}(\eta\text{-}\mathrm{C_7H_7})]^+$ in refluxing acetone with 4-phenyl-1-butyne and 3-phenyl-1-propyne, respectively; these augment the series of known examples (R = H, Ph, Bu^t, Bu^n) and disubstituted $[\mathrm{Mo\{C{=}C(Me)R'\}(dppe)}(\eta\text{-}\mathrm{C_7H_7})]^+$ (R′ = Bu^n, Bu^t).[16] The ambient-temperature ^1H NMR spectra of the vinylidenes **5**–**7** exhibit broad signals for the cycloheptatrienyl ring and the vinylidene substituents characteristic of vinylidene rotation, as demonstrated previously for $[\mathrm{Mo\{C{=}C(H)R\}(dppe)}(\eta\text{-}\mathrm{C_7H_7})]^+$ (R = H, Bu^n); this will be discussed further in a subsequent section.

Although we have previously described cycloheptatrienyl molybdenum vinylidene complexes with supporting ligands other than dppe (i.e. dppm and dmpe),[16] bis(phosphine) complexes of the cycloheptatrienyl molybdenum auxiliary with monodentate P-donor ligands are generally very labile to ligand dissociation,[20] and therefore, analogues of the extensive $\mathrm{Ru(PPh_3)_2Cp}$ series are not readily accessible. However, we have developed a synthesis of $[\mathrm{MoI\{P(OMe)_3\}_2}(\eta\text{-}\mathrm{C_7H_7})]$[37] and now demonstrate that this is a precursor to the vinylidene $[\mathrm{Mo\{C{=}C(H)Ph\}\{P(OMe)_3\}_2}(\eta\text{-}\mathrm{C_7H_7})][\mathrm{BF_4}]$ (**8**). The complex $[\mathrm{MoI\{P(OMe)_3\}_2}(\eta\text{-}\mathrm{C_7H_7})]$ is surprisingly labile to dissociation of iodide in MeOH and reacts at ambient temperature with excess $HC{\equiv}CPh$ in the presence of $K[PF_6]$ to give the required vinylidene **8**, but this species is contaminated with the byproduct $[\mathrm{Mo\{P(OMe)_3\}_3}(\eta\text{-}\mathrm{C_7H_7})]^+$, identified in the mixture by mass and ^1H NMR spectroscopy (*m*/*e* (electrospray) 561; ^1H (CD_2Cl_2) δ 5.28, quadruplet J(P–H) = 3 Hz, C_7H_7; δ 3.63, multiplet, $P(OMe)_3$). The formation of $[\mathrm{Mo\{P(OMe)_3\}_3}(\eta\text{-}\mathrm{C_7H_7})]^+$ was partially controlled by running the reaction at ambient temperature with a large excess of $HC{\equiv}CPh$, but nevertheless the resulting mixture of vinylidene **8** and $[\mathrm{Mo\{P(OMe)_3\}_3}(\eta\text{-}\mathrm{C_7H_7})]^+$ could not be satisfactorily separated. To secure a pure sample of **8**, the crude reaction mixture was treated with KOBu^t in acetone to yield the alkynyl complex $[\mathrm{Mo(C{\equiv}CPh)\{P(OMe)_3\}_2}(\eta\text{-}\mathrm{C_7H_7})]$, which was separated from $[\mathrm{Mo\{P(OMe)_3\}_3}(\eta\text{-}\mathrm{C_7H_7})]^+$ by chromatography on alumina and isolated as a purple oil (*m*/*e* (electrospray) 539; IR(CH_2Cl_2) ν(C≡C) 2049 cm^{-1}). Subsequent protonation with $H[BF_4]\cdot OEt_2$ in diethyl ether led to reformation of **8**, which was isolated as an orange solid. Complex **8** is of significance for the reduced steric demands of the metal auxiliary, and evidence for this is immediately apparent from the broad signal for the C_7H_7 ring in the ambient-temperature ^1H NMR spectrum (see later). An additional feature of the ^1H NMR spectrum is the strongly deshielded resonance for the vinylidene proton (δ 7.10; cf. $[\mathrm{Mo\{C{=}C(H)Ph\}(dppe)}(\eta\text{-}\mathrm{C_7H_7})]^+$, δ 5.57), consistent with data for the related bis(pho-

Table 1. ^{1}H, ^{13}C{^{1}H}, and ^{31}P{^{1}H} NMR Data^a for the Complexes [Mo{(C)$_n$=CR$_2$}(dppe)(η-C$_7$H$_7$)]$^+$ (n = 0−2)

	^{1}H NMR			^{13}C{^{1}H} NMR					
	R$_2$	C$_7$H$_7$	L$_2$	C$_\alpha$	C$_\beta$, C$_\gamma$	R$_2$	C$_7$H$_7$	L$_2$	^{31}P{^{1}H} NMR
1^b	3.01, t (7.5), 2H, H$_B$; 1.51, q, 2H, H$_C$; 4.06, t, 2H (7.3), H$_D$	5.52, t {2.7}	3.73, dt (14.9), {11.3}, 1H; 4.80, dt (14.9), {9.0}, 1H, PCH$_2$; 7.41–8.02 m, PPh$_2$	331.2, t,{18.4}		57.2, C$_B$; 23.1, C$_C$; 82.5, C$_D$	89.3	41.6, t {23.1}, PCH$_2$; 135.8–129.4, PPh$_2$	13.6
2^b	2.69, t (7.3), 2H, H$_B$; 1.46, q, 2H, H$_C$; 4.06, t (7.2), 2H, H$_D$	5.27, t {2.5}	2.39, m, PCH$_2$; 7.62–7.91, PPh$_2$	331.7, t {17.9}		57.2, C$_B$; 23.3, C$_C$; 82.3, C$_D$	89.6	27.9, m, PCH$_2$; 137.2–129.4, PPh$_2$	53.0
3	3.05, t (7.0), 2H, H$_B$; 0.93, q, 2H, H$_C$; 1.33, m, 2H, H$_D$; 3.74, t, 2H (5.8), H$_E$	5.52, t {2.7}	3.63, dt (14.8) {11.3}, 1H; 4.85, dt (14.8) {8.9} 1H, PCH$_2$; 7.38–8.25 m, PPh$_2$	342.1, t {18.2}		48.1, t {5.4}, C$_B$; 16.6, C$_C$; 21.8, C$_D$; 72.2, C$_E$	89.5	41.8, t {23.8}, PCH$_2$; 136.5–129.3, PPh$_2$	10.8
4	2.69, t (7.0), 2H, H$_B$; 1.10, m, 2H, H$_C$; 1.46, m, 2H, H$_D$; 3.76, t, 2H (5.9), H$_E$	5.34, t {2.5}	2.22–2.53, m, PCH$_2$; 7.52–8.20 m, PPh$_2$	342.6, t {18.6}		47.8, C$_B$; 17.0, C$_C$; 21.3, C$_D$; 72.0, C$_E$	89.8	28.2, m, PCH$_2$; 137.9–129.5, PPh$_2$	51.5
5	4.65, br, 1H, C=C*H*R; 1.59, br, 2H; 1.20, br, 2H; H$_C$ and H$_D$; 3.32, br, 2H, H$_E$	5.52	2.79, br, 2H; 2.95, br, 2H, PCH$_2$; 7.23–8.11 m, PPh$_2$	369.5, t {28.7}	116.1, br, C$_\beta$	23.2, 32.5, C$_C$ and C$_D$; 61.1, C$_E$	92.4	26.6, m, PCH$_2$; 134.9–126.0, PPh$_2$	54.3
6	4.65, br, 1H, C=C*H*R; 1.79, br, C*H*$_2$C*H*$_2$Ph; 6.98–8.14, m, CH$_2$CH$_2$*Ph*	5.46, br	2.88, br, PCH$_2$; 6.98–8.14, m, PPh$_2$	368.9, br	115.9, C$_\beta$	35.4, 29.3 (CH$_2$); 137.5–126.7 CH$_2$CH$_2$*Ph*	92.6	26.8, m, PCH$_2$; 137.5–126.7, PPh$_2$	55.4
7	4.70, br, 1H, C=C*H*R; 2.68, br, C*H*$_2$Ph; 7.43–8.01, 6.86, 7.23, m CH$_2$*Ph*	5.24, br	2.68, br, PCH$_2$; 7.43–8.01, m, PPh$_2$	369.9, br	116.4, C$_\beta$	33.3 (*C*H$_2$); 135.1–126.9 CH$_2$*Ph*	92.5	26.9, m, PCH$_2$; 135.1–126.9, PPh$_2$	53.1
8	7.10, t, C=C*H*Ph {15.5} 7.38–7.02, m, C=CH*Ph*	5.80, br	3.80, m (O*Me*)	374.3, t {46.4}	122.1, br, C$_\beta$	135.4, 129.9, 128.2, 127.3, C=CH*Ph*	95.0	53.8 (O*Me*)	138.7
9^c	6.76–7.79, m, Ph	5.27, t {3.8}	2.67, m, 2H, 2.51, m, 2H, PCH$_2$; 6.76–7.79, m, PPh$_2$	285.4, t {33.0}	178.7, t {10.4}, C$_\beta$; 136.3, t {6.1}, C$_\gamma$	133.7–125.9, Ph	89.7	25.4, m, PCH$_2$; 133.7–125.9, PPh$_2$	51.4
10^d	1.45, t {3.0}, Me; 6.71–7.93, m, Ph	5.23, t {3.6}	2.64, br, 2H, 2.40, br, 2H, PCH$_2$; 6.71–7.93, m, PPh$_2$	290.0, t {32.6}	179.8, t {10.2}, C$_\beta$; 137.9, t {6.0}, C$_\gamma$	21.5, t {6.3}, Me; 133.8–126.5, Ph	91.8	27.1, br, PCH$_2$; 133.8–126.5, PPh$_2$	51.9, br

[a] Conditions and abbreviations: 300 MHz (^{1}H), 75 MHz (^{13}C{^{1}H}), 121.5 MHz (^{31}P{^{1}H}) for NMR spectra unless stated otherwise; d = doublet, t = triplet, q = quintet, m = multiplet, br = broad; chemical shifts downfield from SiMe$_4$, coupling constants in Hz, with *J*(H−H) values given in parentheses and *J*(H−P) or *J*(C−P) given in braces; in acetone-d_6 solution unless stated otherwise, withlabeling as in Scheme 1. All spectra were recorded at ambient temperature. [b] ^{13}C NMR spectrum in CD$_2$Cl$_2$. [c] 400 MHz (^{1}H), 100 MHz (^{13}C{^{1}H}), 121.5 MHz (^{31}P{^{1}H}) NMR spectra recorded in CD$_2$Cl$_2$. [d] ^{1}H and ^{13}C{^{1}H} spectra recorded in CDCl$_3$ and ^{31}P{^{1}H} spectrum in CD$_2$Cl$_2$.

Table 2. Comparison of ^{13}C NMR Shifts[a] for C_α in the Cumulenylidene Complexes $[M\{(C)_n{=}CR_2\}]^+$

	$(C)_n{=}CR_2$					
	$\overline{CCH_2CH_2CH_2O}$		$C{=}C(H)Ph$		$C{=}C{=}CPh_2$	
M	$\delta(C_\alpha)$	solvent (ref)	$\delta(C_\alpha)$	solvent (ref)	$\delta(C_\alpha)$	solvent (ref)
Mo(dppe)(η-C_7H_7)	331.7 {17.9}	acetone-d_6 (this work)	372.8 {32}	acetone-d_6 (16)	285.4 {33.0}	CD_2Cl_2 (this work)
Fe(dppe)Cp*	336.6[b] {30}	acetone-d_6 (42)	361.2 {33}	$CDCl_3$ (23)	285.0 {37}	$CDCl_3$ (24)
Ru(dppm)(η-C_9H_7)	300.3 {12.0}	$CDCl_3$ (29)	357.0 {15.2}	CD_2Cl_2 (30)	290.3 {16.8}	CD_2Cl_2 (31)

[a] ^2J(P−C) values in Hz, given in braces. [b] Carbene ligand = C(H)Me.

sphite) vinylidene complexes $[M\{C{=}C(H)Ph\}\{P(OMe)_3\}_2Cp]^+$ (M = Fe,[34] Ru[38]).

The deep purple allenylidene complexes $[Mo(C{=}C{=}CRPh)(dppe)(\eta\text{-}C_7H_7)]^+$ (R = Ph (**9**), Me (**10**)) were synthesized by reaction of $[MoBr(dppe)(\eta\text{-}C_7H_7)]$ with disubstituted propargyl alcohols $HC{\equiv}CCRPh(OH)$ in methanol in the presence of $K[PF_6]$ following the protocol originally developed by Selegue.[28] To our knowledge, these are the first examples of an allenylidene ligand attached to a monometallic molybdenum center, although some allenylidene complexes of chromium and tungsten are known[1,13] and there are a few reports of bimetallic allenylidene molybdenum complexes.[39,40] As observed for related Fe and Ru systems,[24,31] both **9** and **10** were formed as mixtures with yellow complexes tentatively formulated as hydroxyvinylidenes. In the case of the diphenylallenylidene derivative **9**, the byproduct was a very minor component of the reaction mixture and was easily separated by chromatography on alumina. Purification of complex **10** was a significant challenge but, as for the analogous indenyl ruthenium complex,[31] was achieved by careful chromatography on silica. To underline the importance of our improved synthesis of $[MoBr(dppe)(\eta\text{-}C_7H_7)]$, attempts to form the allenylidenes **9** and **10** by reaction of $[Mo(acetone)(dppe)(\eta\text{-}C_7H_7)]^+$ with propargyl alcohols in acetone were totally unsuccessful, leading instead to poorly soluble yellow materials for which microanalytical and mass spectroscopic data were consistent with hydroxyvinylidene products. In both **9** and **10**, the formation of the allenylidene chain is confirmed by the characteristic, infrared-active $\nu(C{=}C{=}C)$ asymmetric stretch, which appears at 1876 cm^{-1} in both complexes. This is toward the low-wavenumber end of typical values[1] but is comparable with data for $[Fe(C{=}C{=}CPh_2)(dppe)Cp^*][PF_6]$ ($\nu(C{=}C{=}C)$, Nujol, 1896 cm^{-1})[24] and $[Fe(C{=}C{=}CPh_2)(CO)_2\{P(OMe)_3\}_2]$ ($\nu(C{=}C{=}C)$, hexane, 1868 cm^{-1}).[41]

The availability of a sequence of metallacumulenylidene complexes $[Mo\{(C)_n{=}CR_2\}(dppe)(\eta\text{-}C_7H_7)]^+$ ($n = 0-2$) allows a comparison of spectroscopic and structural data both within the cycloheptatrienyl molybdenum series and with analogous group 8 systems $[M\{(C)_n{=}CR_2\}L_2(\eta\text{-}C_xH_y)]^+$ ($n = 0-2$; M = Fe, Ru; L_2 = 2 PR_3, dppe; C_xH_y = Cp, Cp*, indenyl). The ^{13}C NMR chemical shift data for C_α (Tables 1 and 2) show a strong dependence upon n in the series $[Mo\{(C)_n{=}CR_2\}(dppe)(\eta\text{-}C_7H_7)]^+$ with the following ordering for $\delta(C_\alpha)$: $n = 1 > n = 0 > n = 2$. This sequence is consistent with representative analogues of the $[M\{(C)_n{=}CR_2\}L_2(\eta\text{-}C_xH_y)]^+$ (M = Fe, Ru) series (Table 2) and reflects the very strong electron acceptor capacity of the vinylidene ligand. For a given value of n, the $\delta(C_\alpha)$ values fall within a narrow range, even for the different metal centers, Mo, Fe, and Ru, but it is notable that chemical shifts are sensitive to ring size in oxacyclocarbenes and that the $\delta(C_\alpha)$ value of ca. 370 ppm, typical of vinylidene derivatives of the $MoL_2(\eta\text{-}C_7H_7)$ auxiliary, is close to the low-field limit of normal values.[6] All resonances for C_α are observed as triplets due to ^2J(P−C) coupling to the P-donor ligand L_2, but in general ^2J(P−C) values for the Ru complexes are only half of those observed for the Fe and Mo analogues. In the allenylidene complexes **9** and **10**, C_α, C_β, and C_γ each appear as a triplet resonance; the chemical shift order $C_\alpha > C_\beta > C_\gamma$ is assumed, consistent with assignments for $[M(C{=}C{=}CR_2)L_2(\eta\text{-}C_xH_y)]^+$ (R = alkyl, aryl; M = Fe, L_2 = dppe, C_xH_y = Cp*;[24] M = Ru, L_2 = 2PPh_3, C_xH_y = indenyl[31]).

Structural Studies. We have previously described four structural studies on the $[Mo\{(C)_n{=}CR_2\}(dppe)(\eta\text{-}C_7H_7)]^+$ series comprising the oxacyclocarbene $[Mo(\overline{CCH_2CH_2CH_2O})(dppe)(\eta\text{-}C_7H_7)]^+$ (**2**)[21]and the three vinylidene complexes $[Mo\{C{=}C(R)R'\}(dppe)(\eta\text{-}C_7H_7)]^+$ (R = H, R′ = Ph,[16] $(CH_2)_3OH$ (**5**);[21] R = Ph, R′ = $Mo\{C{=}CPh\}(dppe)(\eta\text{-}C_7H_7)$[16]). An intriguing feature of this work is the orientation of the cumulenylidene ligand R substituents with repect to the pseudo mirror plane which bisects the $Mo(dppe)(\eta\text{-}C_7H_7)$ fragment. Thus, the oxacarbene ring of **2** is disposed orthogonal to the mirror plane in a horizontal alignment, whereas in each of the vinylidene complexes, the R substituents lie in the mirror plane and are assigned to a vertical configuration. The 90° twist of R substituents for each integer increase in n is consistent with the bonding in the cumulenylidene ligand series, but what is unexpected is the observed ligand orientation. Structural studies on the $[M\{(C)_n{=}CR_2\}L_2(\eta\text{-}C_xH_y)]^+$ ($n = 0-2$; M = Fe, Ru) series reveal that carbenes adopt a vertical configuration,[27,42,43] vinylidenes are horizontal,[24,30,43] and allenylidenes exhibit a vertical arrangement of R substituents.[24,28,31] In terms of the benchmark, self-consistent-field (SCF) calculations on these systems,[44] it appears therefore that preferred plane of the π interaction of the $Mo(dppe)(\eta\text{-}C_7H_7)$ auxiliary with the vacant p orbital of the cumulenylidene ligand is the converse of that in the $[M\{(C)_n{=}CR_2\}L_2(\eta\text{-}C_xH_y)]^+$ (M = Fe, Ru) series. However, considerable care must be exercised in reaching this conclusion, because the energy difference between horizontal and vertical configurations is often relatively small and steric considerations can override electronic factors. The purpose of the current structural work was therefore to provide additional evidence for a genuine electronic preference of the $Mo(\eta\text{-}C_7H_7)$ system by (i) examination of the vinylidene ligand orientation in the less sterically demanding environment of $[Mo\{C{=}C(H)Ph\}\{P(OMe)_3\}_2(\eta\text{-}C_7H_7)][BF_4]$ (**8**) and (ii) demonstration of successive 90° twists of ligand R substituents across the extended

---

(38) Bruce, M. I.; Cifuentes, M. P.; Snow, M. R.; Tiekink, E. R. T. *J. Organomet. Chem.* **1989**, *359*, 379.

(39) Froom, S. F. T.; Green, M.; Mercer, R. J.; Nagle, K. R.; Orpen, A. G.; Rodrigues, R. A. *J. Chem. Soc., Dalton Trans.* **1991**, 3171.

(40) Capon, J.-F.; Le Berre-Cosquer, N.; Leblanc, B.; Kergoat, R. J. *Organomet. Chem.* **1996**, *508*, 31.

(41) Gauss, C.; Veghini, D.; Orama, O.; Berke, H. *J. Organomet. Chem.* **1997**, *541*, 19.

(42) Mahias, V.; Cron, S.; Toupet, L.; Lapinte, C. *Organometallics* **1996**, *15*, 5399.

(43) Bruce, M. I.; Humphrey, M. G.; Snow, M. R.; Tiekink, E. R. T. *J. Organomet. Chem.* **1986**, *314*, 213.

(44) Kosti, N. M.; Fenske, R. F. *Organometallics* **1982**, *1*, 974.

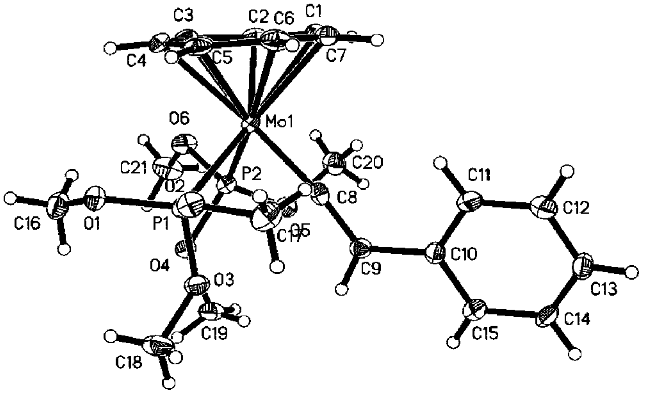

Figure 1. Molecular structure of complex **8** (counteranion and solvent of crystallization omitted). Thermal ellipsoids are given at the 50% probability level.

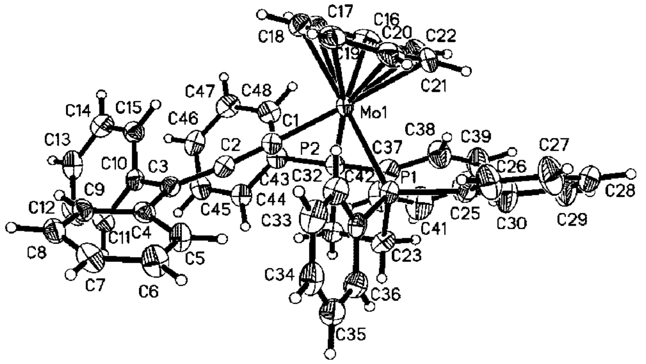

Figure 2. Molecular structure of complex **9** (counteranion and solvent of crystallization omitted). Thermal ellipsoids are given at the 50% probability level.

Table 3. Important Bond Lengths (Å) and Angles (deg)[a]

	Complex **8**		
Mo(1)−P(1)	2.4613(7)	Mo(1)−C(2)	2.311(3)
Mo(1)−P(2)	2.4653(7)	Mo(1)−C(3)	2.363(3)
Mo(1)−C(8)	1.929(3)	Mo(1)−C(4)	2.356(3)
C(8)−C(9)	1.327(4)	Mo(1)−C(5)	2.287(3)
C(9)−C(10)	1.469(4)	Mo(1)−C(6)	2.334(3)
Mo(1)−C(1)	2.327(3)	Mo(1)−C(7)	2.316(3)
P(1)−Mo(1)−P(2)	91.61(3)	Mo(1)−C(8)−C(9)	172.4(2)
P(1)−Mo(1)−C(8)	79.62(8)	C(8)−C(9)−C(10)	126.8(2)
P(2)−Mo(1)−C(8)	80.88(8)	Ct−Mo(1)−C(8)	138.7
	Complex **9**		
Mo(1)−P(1)	2.5132(9)	Mo(1)−C(22)	2.355(4)
Mo(1)−P(2)	2.5102(9)	Mo(1)−C(16)	2.284(4)
Mo(1)−C(1)	1.994(3)	Mo(1)−C(17)	2.313(4)
C(1)−C(2)	1.258(5)	Mo(1)−C(18)	2.302(4)
C(2)−C(3)	1.354(5)	Mo(1)−C(19)	2.316(4)
C(3)−C(4)	1.479(5)	Mo(1)−C(20)	2.301(4)
Mo(1)−C(21)	2.321(4)	Mo(1)−C(21)	2.321(4)
P(1)−Mo(1)−P(2)	78.34(3)	C(1)−C(2)−C(3)	174.4(4)
P(1)−Mo(1)−C(1)	84.01(10)	C(2)−C(3)−C(4)	121.1(3)
P(2)−Mo(1)−C(1)	77.46(10)	C(2)−C(3)−C(10)	119.1(3)
Mo(1)−C(1)−C(2)	176.1(3)	Ct−Mo(1)−C(1)	131.6

[a] Ct = centroid of C_7H_7 ring.

series $[Mo\{(C)_n{=}CR_2\}(dppe)(\eta\text{-}C_7H_7)]^+$ ($n = 0{-}2$) via determination of the structure of the allenylidene complex $[Mo(C{=}C{=}CPh_2)(dppe)(\eta\text{-}C_7H_7)][PF_6]$ (**9**).

The X-ray crystal structures of $[Mo\{C{=}C(H)Ph\}\{P(OMe)_3\}_2(\eta\text{-}C_7H_7)][BF_4].MeOH$ (**8**) and $[Mo(C{=}C{=}CPh_2)(dppe)(\eta\text{-}C_7H_7)][PF_6]\cdot 0.25CH_2Cl_2$ (**9**), together with the crystallographic numbering schemes, are illustrated in Figures 1and 2, respectively; important bond lengths and angles are given in Table 3. The availability of structural data for the extended series $[Mo\{(C)_n{=}CR_2\}(dppe)(\eta\text{-}C_7H_7)]^+$ ($n = 0{-}2$) permits an examination of the dependence of the $Mo{-}C_\alpha$ bond length upon the identity of the cumulenylidene ligand, and a summary of data for the Mo, Fe, and Ru series is presented in Table 4. In all cases, the $M{-}C_\alpha$ distance is shortest for the vinylidene complex, consistent with the strong acceptor capacity of this ligand. The $M{-}C_\alpha$ distances for carbene and allenylidene complexes are very similar, although the seemingly longer $Mo{-}C_\alpha$ distances determined for the two independent molecules of the cyclooxacarbene **2** (2.02(3), 2.04(3) Å)[21] are consistent with those reported for *trans*-$[MoI(\overline{CCH_2CH_2CH_2O})(CO)_2(\eta\text{-}C_5R_5)]$ (R = H, 2.068(8) Å;[45] R = Me, 2.040(20) Å[46]). The vinylidene ligand of **8** and allenylidene ligand of **9** exhibit $C_\alpha{-}C_\beta$ and $C_\beta{-}C_\gamma$ bond lengths within normal ranges; the significant shortening of $C_\alpha{-}C_\beta$ (C(1)-C(2)) in **9** is consistent with a contribution from the canonical form $[M^-]{-}(C{\equiv}CC^+Ph_2)$.[1] However, the principal structural feature of interest in **8** and **9** is the orientation of the cumulenylidene ligand. In **8**, the vinylidene ligand adopts a vertical configuration with the more bulky Ph substituent located in the "up" position, directed toward the cycloheptatrienyl ring in accord with the structures of $[Mo\{C{=}C(H)R\}(dppe)(\eta\text{-}C_7H_7)]^+$ (R = Ph, $(CH_2)_3OH$). The dihedral angle between the planes defined by Ct−Mo−C(8) and C(8)−C(9)−C(10) (Ct represents the centroid of the cycloheptatrienyl ring) is 9.3° in **8** (cf. $[Mo\{C{=}C(H)Ph\}(dppe)(\eta\text{-}C_7H_7)][BF_4]$, 10.6°), indicating a small deviation from the precise vertical configuration; such departures from "ideal" configurations are common for metallacumulenylidenes of the type $[M\{(C)_n{=}CR_2\}L_2(\eta\text{-}C_xH_y)]^+$ ($n = 0{-}2$; M = Fe, Ru) with dihedral angles typically in the range 10–30°. In contrast to the vertical configuration of the vinylidene in complex **8**, the allenylidene ligand of **9** adopts a horizontal arrangement with negligible divergence from an ideal configuration (the dihedral angle between planes defined by Ct−Mo(1)−C(1) and C(2)−C(3)−C(4)−C(5) is 89.5°). The horizontal orientation of the allenylidene ligand in **9** completes the data set for $[Mo\{(C)_n{=}CR_2\}(dppe)(\eta\text{-}C_7H_7)]^+$ ($n = 0{-}2$) and confirms the predictions based on carbene (horizontal) and vinylidene (vertical) complexes. In summary, therefore, the new structural work, together with previous studies on $[Mo(\overline{CCH_2CH_2CH_2O})(dppe)(\eta\text{-}C_7H_7)]^+$ and $[Mo\{C{=}C(H)R'\}(dppe)(\eta\text{-}C_7H_7)]^+$, now strongly suggests that the $MoL_2(\eta\text{-}C_7H_7)$ auxiliary has a clear electronic preference for π interaction with the vacant p orbital on the cumulenylidene $C_\alpha$carbon, which is the converse of that found for analogous group 8 auxiliaries. Although examples of horizontally orientated carbene[47] and vertical vinylidene[17] ligands in half-sandwich complexes are known, the work on the $MoL_2(\eta\text{-}C_7H_7)$ auxiliary reported here represents a unique case in which these atypical orientations are linked in a single system with a proven, systematic 90° rotation of the R substituents with each additional cumulenylidene ligand carbon.

---

(45) Bailey, N. A.; Chell, P. A.; Manuel, C. P.; Mukhopadhyay, A.; Rogers, D.; Tabbron, H.; Winter, M. J. *J. Chem. Soc., Dalton Trans.* **1983**, 2397.

(46) Bailey, N. A.; Dunn, D. A.; Foxcroft, C. N.; Harrison, G. R.; Winter, M. J.; Woodward, S. J. *J. Chem. Soc., Dalton Trans.* **1988**, 1449.

(47) Riley, P. E.; Davis, R. E.; Allison, N. T.; Jones, W. M. *Inorg. Chem.* **1982**, *21*, 1321.

Table 4. Comparison of M−C$_\alpha$ Distances (Å) for Carbene, Vinylidene, and Allenylidene Complexes of the Type [M{(C)$_n$=CR$_2$}L$_2$(η-C$_x$H$_y$)]$^+$

[Mo{(C)$_n$=CR$_2$}(dppe)(η-C$_7$H$_7$)]$^+$		[Fe{(C)$_n$=CR$_2$}(dppe)Cp*]$^+$		[Ru{(C)$_n$=CR$_2$}(PPh$_3$)$_2$(η-C$_9$H$_7$)]$^+$	
(C)$_n$=CR$_2$	Mo−C$_\alpha$ (Å)	(C)$_n$=CR$_2$	Fe−C$_\alpha$ (Å)	(C)$_n$=CR$_2$	Ru−C$_\alpha$ (Å)
$\overline{CCH_2CH_2CH_2O}$	2.04(3), 2.02(3)[21]	C(H)Me	1.787(8)[42]	$\overline{CCH_2(CH_2)_3CH_2O}$	1.89(1)[29]
C=C(H)Ph	1.93(1)[16]	C=C(H)Ph	1.760(5)[24]	C=CMe$_2$	1.839(7)[30]
C=C=CPh$_2$	1.994(3)	C=C=CPh$_2$	1.785(5)[24]	C=C=CPh$_2$	1.878(5)[31]

Dynamic NMR Investigations. Variable-temperature ^{1}H and ^{31}P{^{1}H} NMR studies on complexes of the type [M{(C)$_n$=CR(R′)}L$_2$(η-C$_x$H$_y$)]$^+$ (n = 0, 1; M = Fe, Ru) have been usefully exploited to establish low-temperature solution conformations and activation energies to carbene[48–50] and vinylidene ligand[22,51,52] rotation. In examples where the cumulenylidene ligand adopts a low-temperature, horizontal orientation, complexes of the formulation [M{(C)$_n$=CR(R′)}L$_2$(η-C$_x$H$_y$)]$^+$ (R ≠ R′) exist as two enantiomers and the inequivalent, diastereotopic phosphorus atoms of the supporting ligand L$_2$ can be distinguished by ^{31}P{^{1}H} NMR spectroscopy. By contrast, where a vertical orientation is adopted, complexes [M{(C)$_n$=CR(R′)}L$_2$(η-C$_x$H$_y$)]$^+$ (R ≠ R′) can, in principle, exist as two diastereomers at low temperature in which either R or R′ points up toward the C$_x$H$_y$ ring. The two enantiotopic phosphorus atoms of each individual rotamer are indistinguishable by ^{31}P{^{1}H} NMR spectroscopy, but each rotamer gives rise to discrete sets of resonances in both ^{31}P and ^{1}H NMR spectra.[22] Because the Mo(dppe)(η-C$_7$H$_7$) auxiliary promotes cumulenylidene ligand orientations which are the converse of those of the widely explored cyclopentadienyl iron/ruthenium analogues, it consequently provides new opportunities for dynamic NMR investigations.

First considered are variable-temperature NMR studies on the carbene complex [Mo{$\overline{CCH_2CH_2CH_2O}$}(dppe)(η-C$_7H_7$)]$^+$ (**2**) and the allenylidene [Mo(C=C=CMePh)(dppe)(η-C$_7$H$_7$)]$^+$ (**10**). Both of these complexes are expected to adopt a preferred horizontal orientation on the basis of structural studies and should therefore be accessible to investigations by ^{31}P{^{1}H} NMR spectroscopy. The ^{31}P{^{1}H} NMR spectrum of the carbene complex **2** exhibited only a temperature-independent singlet resonance in the range 190–300 K. However, the dynamic behavior of the allenylidene **10** was much more informative and the broad singlet observed in the ambient-temperature ^{31}P{^{1}H} NMR spectrum resolved on cooling to a doublet of doublets pattern arising from the inequivalent phosphorus atoms syn to the Me and Ph substituents of a horizontal allenylidene ligand. The coalescence temperature (T_c) for the process was determined as 290 K, giving an estimated barrier to rotation of the allenylidene ligand in **10** of 57.8 kJ mol^{-1}; this should be compared with the data for the related vinylidene [Mo{C=CH$_2$}(dppe)(η-C$_7$H$_7$)]$^+$, (51.9 kJ mol^{-1}, T_c = 268 K),[16] for which the cumulenylidene ligand substituents are much smaller but less remote from the metal center. The experimental estimation of a barrier to rotation of the allenylidene ligand in complex **10** is a key result of this work, realized by the specific properties of the Mo(dppe)(η-C$_7$H$_7$) auxiliary. There have been very few reports on the determination of rotation barriers for cumulenylidene ligands with $n > 1$, and to our knowledge, for the allenylidene ligand, there is only one previous account which relates to [Ru(C=C=CPhFc)(dppf)Tp]$^+$ (Fc = ferrocenyl, dppf = bis(diphenylphosphino)ferrocene, Tp = HB(pz)$_3$).[53] Although not demonstrated crystallographically, this complex also adopts a horizontal orientation of the allenylidene ligand, as established by variable-temperature ^{31}P{^{1}H} NMR studies, and the barrier to allenylidene rotation was estimated as 47 kJ mol^{-1} (for T_c = 238 K).

Vinylidene complexes of the type [Mo{C=C(R)R′}(dppe)(η-C$_7$H$_7$)]$^+$ adopt a preferred vertical orientation of the vinylidene ligand at low temperature, and therefore, in principle, for R ≠ R′ two diastereomers are observed, dependent upon the relative positions of R and R′ with respect to the C$_7$H$_7$ ring. We have previously described variable-temperature ^{1}H and ^{31}P{^{1}H} NMR investigations on [Mo{C=C(R)R′}(dppe)(η-C$_7$H$_7$)]$^+$ (R = H, R′ = H, Ph, Bu^n, Bu^t; R = Me, R′ = Bu^n, Bu^t)[16] and made the following observations: (i) the NMR spectra of the derivatives (R = H, R′ = H, Bu^n) are temperature dependent, indicating vinylidene rotation on the NMR time scale; (ii) the remaining derivatives (R = H, R′ = Ph, Bu^t; R = Me, R′ = Bu^n, Bu^t) exhibit temperature-independent spectra, and (with the single exception of R = Me, R = Bu^n) there is no evidence for the coexistence of two diastereomers, only one singlet signal being observed in the ^{31}P{^{1}H} NMR spectra. Although these latter results could be mostly explained by rapid rotation about the Mo−C$_\alpha$ bond, a more probable rationalization is that in [Mo{C=CRR′}(dppe)(η-C$_7$H$_7$)]$^+$ (R = H, R′ = Ph, Bu^t; R = Me, R′ = Bu^t) the barrier to vinylidene rotation is relatively high and, at low temperature, the complexes assume a single preferred structure in which the sterically more demanding vinylidene substituent is located syn to the cycloheptatrienyl ring. This proposed selectivity in vinylidene ligand orientation, imposed by the Mo(dppe)(η-C$_7$H$_7$) auxiliary, has potential applications in stereoselective synthesis, and therefore, further studies to account for the temperature independence of the NMR spectra of [Mo{C=C(R)R′}(dppe)(η-C$_7$H$_7$)]$^+$ (R = H, R′ = Ph, Bu^t; R = Me, R′ = Bu^t) were undertaken.

As described in Synthetic Studies, the series of vinylidenes [Mo{C=C(H)(CH$_2$)$_x$Ph}L$_2$(η-C$_7$H$_7$)]$^+$ (L$_2$ = dppe, x = 2 (**6**), 1 (**7**); L$_2$ = 2 P(OMe)$_3$, x = 0 (**8**)) have been designed for this investigation. The purpose of the dppe series is to monitor the effect of progressive reduction of the methylene spacer chain between the vinylidene C$_\beta$ and the phenyl substituent; the P(OMe)$_3$ complex **8** permits investigation of the effect of changing the steric control of the supporting L$_2$ ligand(s) (dppe vs 2 P(OMe)$_3$). The results of variable-temperature ^{1}H and ^{31}P{^{1}H} NMR investigations on complexes **6**−**8** are summarized in Table 5. At ambient temperature, all three complexes exhibit broadened ^{1}H NMR signals which sharpen on cooling to two discrete sets of resonances; a full spectral assignment was not made, due to the complex overlap of resonances, but the signals assignable to the C$_7$H$_7$ ring protons for the two individual diastereomers were clearly resolved in all cases. In the ^{31}P{^{1}H} NMR spectra, complexes **6**−**8** each exhibit a singlet at room temperature but cooling resulted in resolution into two singlet

---

(48) Brookhart, M.; Tucker, J. R.; Flood, T. C.; Jensen, J. *J. Am. Chem. Soc.* **1980**, *102*, 1203.

(49) Studabaker, W. B.; Brookhart, M. *J. Organomet. Chem.* **1986**, *310*, C39.

(50) Roger, C.; Lapinte, C. *J. Chem. Soc., Chem. Commun.* **1989**, 1598.

(51) Consiglio, G.; Morandini, F. *Inorg. Chim. Acta* **1987**, *127*, 79.

(52) Gamasa, M. P.; Gimeno, J.; Lastra, E.; Martín, B. M.; Anillo, A.; Tiripicchio, A. *Organometallics* **1992**, *11*, 1373.

(53) Hartmann, S.; Winter, R. F.; Brunner, B. M.; Sarkar, B.; Knödler, A.; Hartenbach, I. *Eur. J. Inorg. Chem.* **2003**, 876.

Table 5. Key Low-Temperature ^{1}H and ^{31}P{^{1}H} NMR Data for Vinylidene and Allenylidene Complexes [a]

			^{1}H NMR		^{31}P{^{1}H} NMR	
complex	temp (°C)	isomer	δ(C$_7$H$_7$)	major:minor isomer distribn (%)	δ(^{31}P)	major:minor isomer distribn (%)
6	−60	major	5.44, t {3.0}	66	56.5	66
		minor	5.32, t {3.0}	34	55.4	34
7	−60	major	5.27	91	53.5	93
		minor	5.36	9	52.9	7
8	−60	major	5.86, t {4.4}	95	140.2	94
		minor	5.72, t {4.2}	5	141.7	6
10[b]	−40				53.0, d (14); 52.2, d (14)	

[a] Conditions and abbreviations: 300 MHz (^{1}H), 121.5 MHz (^{31}P{^{1}H}) NMR spectra; all signals singlets unless stated otherwise; d = doublet, t = triplet; chemical shifts downfield from SiMe$_4$; coupling constants in Hz, *J*(H−P) values given in braces, *J*(P−P) values given in parentheses; in acetone-*d*$_6$ solution unless stated otherwise. [b] ^{31}P{^{1}H} NMR spectrum in CD$_2$Cl$_2$.

signals of different intensity, again arising from the two possible rotameric forms. Isomer ratios at −60 °C were calculated from integrals of both the ^{1}H (C$_7$H$_7$ resonances) and ^{31}P{^{1}H} NMR spectra and good agreement obtained between the two methods (see Table 5). It is clear that reduction of the methylene spacer chain in [Mo{C=C(H)(CH$_2$)$_x$Ph}(dppe)(η-C$_7$H$_7$)]$^+$ from $x = 2$ (**6**) to $x = 1$ (**7**) has a major effect on isomer ratios, with the vast majority of complex **7** existing as one isomer at −60 °C; an extension of this trend to $x = 0$ therefore points toward a single form of [Mo{C=C(H)Ph}(dppe)(η-C$_7$H$_7$)]$^+$ in solution at low temperature. The variable-temperature behavior of complex **8** is significant in that reduction in the steric demands of the supporting L$_2$ ligand set permits observation of two rotamers at low temperature, even with no methylene spacer between C$_\beta$ and the phenyl ring. However, once again, one isomer is predominant and it is likely that an increase in the bulk of L$_2$ will further this trend. In summary, it is probable that the temperature -independent behavior of the NMR spectra of the vinylidenes [Mo{C=C(R)R′}(dppe)(η-C$_7$H$_7$)]$^+$ (R = H, R′ = Ph, Bu^t; R = Me, R′ = Bu^t) can be attributed to the existence of a single preferred isomer in solution at low temperature. We cannot exclude vinylidene rotation at ambient temperature in these complexes, but the well-resolved, sharp resonances observed (in contrast to **6**−**8**) are indicative of high energy barriers and slow rotation.

Theoretical Investigations. For a more detailed insight into the origin of the inverse orientational preferences of cumulenylidene ligands attached to Mo(dppe)(η-C$_7$H$_7$) and Ru(dppe)Cp auxiliaries, quantum-chemical calculations were carried out on the unsubsituted vinylidenes [Mo(C=CH$_2$)(dppe)(η-C$_7$H$_7$)]$^+$ (**11**) and [Ru(C=CH$_2$)(dppe)Cp]$^+$ (**12**) to effect a direct comparison of the two systems. The investigation was then extended to the allenylidene [Mo(C=C=CMePh)(dppe)(η-C$_7$H$_7$)]$^+$ (**10**) to examine the effect of increase in cumulenylidene chain length. To our knowledge, there are very few previous reports of DFT calculations carried out on the Mo(η-C$_7$H$_7$) system.[54,55]

The calculations were performed with the Gaussian 03 suite of programs,[56] and all structures were characterized by frequency analysis. Full geometry optimizations were performed with a variety of basis sets: the 3-21G* all-electron basis, the LANL2DZ relativistic core potential for Mo coupled with Dunning's double-ζ set for H, C, and P, and the SDD effective core potentials for all atoms (except H). These basis sets are probably not sufficiently large for quantitative accuracy but are sufficient to explore the geometric and electronic changes within these systems. Furthermore, the size of these systems makes the use of very large basis sets unfeasible. Three exchange-correlation functionals were used: B3LYP, B3PW91, and BP86. Having obtained the minimum energy structures for **10**−**12**, a rigid rotation of the C=CH$_2$ unit in **11** and the C=C=C(Me)Ph unit in **10** was carried out to obtain the approximate location of the transition states for rotation in each system. Starting from these approximate transition-state geometries, full optimizations were performed to properly locate the saddle-point structures.

We find that the barrier for rotation is underestimated at all levels. This is a trend often observed in density functional calculations. It is possible to refine these methods for specific purposes by varying the exchange functional, but we have chosen not to do so here. When zero-point and thermal energy corrections are included, all levels except BP86/LANL2DZ predict the rotational barrier in **10** to be lower than that in **11**. At the BP86/LANL2DZ level both **10** and **11** are predicted to have a free energy of activation of 45 kJ mol^{-1}, which is still too low relative to the barriers observed in the dynamic NMR experiments (**10**, 57.8 kJ mol^{-1}; **11**, 51.9 kJ mol^{-1}). The rotational barrier in the Ru system, **12**, is calculated to be significantly smaller at 34 kJ mol^{-1}, in line with the value reported for [Ru{C=C(H)Ph}(dppe)Cp]$^+$ (38 kJ mol^{-1}).[51]

The calculated structures for **10**−**12**, described below, exhibit cumulenylidene ligand orientations fully consistent with experimental, structural data. In **11**, the plane of the C=CH$_2$ unit makes a dihedral angle with the Mo−Ct vector (where Ct = centroid of the C$_7$H$_7$ ring) of 4.0°. In the rotational transition state this dihedral angle becomes 91.5°. In contrast, for the Ru system **12**, the plane of the C=CH$_2$ unit makes a dihedral angle with the Ru−Ct$_2$ vector (where Ct$_2$ = centroid of the C$_5$H$_5$ ring) of 79.9° at equilibrium and 5.5° in the rotational transition state. In **10**, the orientation of the C$_3$ unit follows the behavior in **12** with the end unit rotated so that the dihedral angle between the C=C=C(Me)Ph plane and the Mo−Ct vector is 75.4° and reduces to 0.5° in the rotational transition state.

To investigate the electronic changes which occur on forming the rotational transition state, and to understand the orientational preferences, we need to consider the frontier molecular orbitals

---

(54) Menconi, G.; Kaltsoyannis, N. *Organometallics* **2005**, *24*, 1189.

(55) Tamm, M.; Dressel, B.; Lügger, T.; Fröhlich, R.; Grimme, S. *Eur. J. Inorg. Chem.* **2003**, 1088.

(56) Frisch, M. J.; Trucks, G. W.; Schlegel, H. B.; Scuseria, G. E.; Robb, M. A.; Cheeseman, J. R.; Montgomery, J. A.; Jr., Vreven, T.; Kudin, K. N.; Burant, J. C.; Millam, J. M.; Iyengar, S. S.; Tomasi, J.; Barone, V.; Mennucci, B.; Cossi, M.; Scalmani, G.; Rega, N.; Petersson, G. A.; Nakatsuji, H.; Hada, M.; Ehara, M.; Toyota, K.; Fukuda, R.; Hasegawa, J.; Ishida, M.; Nakajima, T.; Honda, Y.; Kitao, O.; Nakai, H.; Klene, M.; Li, X.; Knox, J. E.; Hratchian, H. P.; Cross, J. B.; Bakken, V.; Adamo, C.; Jaramillo, J.; Gomperts, R.; Stratmann, R. E.; Yazyev, O.; Austin, A. J.; Cammi, R.; Pomelli, C.; Ochterski, J. W.; Ayala, P. Y.; Morokuma, K.; Voth, G. A.; Salvador, P.; Dannenberg, J. J.; Zakrzewski, V. G.; Dapprich, S.; Daniels, A. D.; Strain, M. C.; Farkas, O.; Malick, D. K.; Rabuck, A. D.; Raghavachari, K.; Foresman, J. B.; Ortiz, J. V.; Cui, Q.; Baboul, A. G.; Clifford, S.; Cioslowski, J.; Stefanov, B. B.; Liu, G.; Liashenko, A.; Piskorz, P.; Komaromi, I.; Martin, R. L.; Fox, D. J.; Keith, T.; Al-Laham, M. A.; Peng, C. Y.; Nanayakkara, A.; Challacombe, M.; Gill, P. M. W.; Johnson, B.; Chen, W.; Wong, M. W.; Gonzalez, C.; Pople, J. A. *Gaussian 03, Revision C.02*; Gaussian, Inc., Wallingford, CT, 2004.

involved. To aid the analysis, we have adopted an approach loosely based on the work of Kostić and Fenske.[44] We have not been able to find explicit expressions for the molecular orbital decomposition used in ref 44; hence, we have used the following procedure. Each molecule was divided into two fragments. In **10**, the fragments were (C=C=CMePh) and $[\text{Mo(dppe)}(\eta\text{-C}_7\text{H}_7)]^+$, while in **11** and **12** they were (C=CH_2) and $[\text{Mo(dppe)}(\eta\text{-C}_7\text{H}_7)]^+$ or $[\text{Ru(dppe)Cp}]^+$, respectively. Calculations on all fragments were carried out separately. Provided that the ordering and orientation of the atoms are the same in the fragments as in the complete system, we can then form a block diagonal matrix of molecular orbital coefficients of the fragments, $\mathbf{C_F}$. We then calculate the molecular orbital coefficient for the complete system, $\mathbf{C_T}$, and look for the transformation, **T**, that expresses the molecular orbital of the complete system as a linear combination of the fragment molecular orbitals: $\mathbf{C_T} = \mathbf{C_F T}$. The transformation matrix **T** is formed as $T = \mathbf{C_F}^{-1}\mathbf{C_T}$. The columns of **T** are then normalized such that $\sum_j |T_{ji}| = 1$. Hence, each column of **T** gives the composition of the corresponding molecular orbital of the complete system as a linear combination of the fragment molecular orbitals. This type of analysis is helpful in identifying the nature of the orbitals involved, but when used with larger than minimal basis sets, it is found that the weights of the fragment orbitals are quite small and there are many contributions of similar weight. In combination with this technique we have also employed population analysis and the Pipek−Mezey localization method[57] to build a picture of the salient bonding interactions in these systems.

Starting with $[\text{Mo(C=CH}_2\text{)(dppe)}(\eta\text{-C}_7\text{H}_7)]^+$ (**11**), we find the frontier orbitals shown in Figure 3. Note that the HOMO of the $\text{H}_2\text{C=C}$ unit is the carbene-like orbital which will participate in σ bonding to the Mo; obviously this cannot influence the orientational preference, and so we concentrate here on the π bonding between the Mo and the C=CH_2 unit. The axes are oriented such that the C=CH_2 unit lies in the *yz* plane. In the Mo-containing fragment, the HOMO is a d_{z^2} orbital directed to the center of the C_7H_7 ring. The HOMO-1 is a d_{xy} orbital involved in a δ bond with the C_7H_7 ring. Similarly, HOMO-2 appears to lie in the *xy* plane (but directed along the axes) and forms a δ bond with the C_7H_7 ring, but the orbital is tilted relative to the ring. It should be borne in mind that these orbitals will remix in the presence of the C=CH_2 unit so that there is optimal alignment of orbitals between fragments. Furthermore, the $\text{Mo−C}_7\text{H}_7$ orbital interactions will alter as the metal orbitals tilt from the ring. Turning to the orbitals of the complete system **11**, we find the lowest π bonding orbital (HOMO-11) to be a mixture of a d_{xy} orbital on Mo coupled with the π bonding orbital of C=CH_2. The other π interactions (HOMO-2 and HOMO-1) appear to be dominated by the LUMO of the C=CH_2 unit. HOMO-1 in **11** is a bonding interaction between the metal HOMO (now tilted and interacting with the C_7H_7 ring) and the LUMO of C=CH_2. The calculated Ct−Mo−CCH_2 angle is 134.1°, and this accommodates the successful interaction between these orbitals (note the experimental value of 135° reported for $[\text{Mo(C=CHPh)(dppe)}(\eta\text{-C}_7\text{H}_7)][\text{BF}_4]$).[16] HOMO-2 in **11** is again a bonding interaction between a filled metal orbital and the LUMO of C=CH_2.

Given that, in **10**, the preferred orientation of the C=C=CR_2 unit is opposite to that of the C=CR_2 unit in **11** and the metal -containing fragments are the same, the orientation must be dictated by the orbitals of the vinylidene or allenylidene ligand, respectively. The previous discussion suggests that the orbitals responsible for directing the orientation are the HOMO of the metal fragment and the LUMO of the cumulenylidene ligand. With this in mind, we now consider the orbitals of $[\text{Ru(C=CH}_2\text{)(dppe)Cp}]^+$ (**12**), shown in Figure 4. The most notable difference is that the HOMO of the metal-containing fragment is now the d_{xy} orbital of Ru, which is perpendicular to the HOMO of **11**; the LUMO of the C=CH_2 unit is of course the same. The π bonding orbitals of the Ru−C=CH_2 unit now lie somewhat lower in the manifold but are clearly identifiable. These orbitals are HOMO-2 and HOMO-10. In both cases we again see a clear interaction between the Ru orbitals in the *xy* plane and the LUMO of the C=CH_2 unit. Thus, the bonding interaction that explained the orientation in **11** also seems to explain the orientation in **12**. We also note that the lowest lying π interaction is HOMO-13. This orbital is a bonding combination of the π bonding orbital on C=CH_2 and the LUMO on the metal fragment. The antibonding combination of these orbitals appears as the HOMO in **12** (the corresponding orbitals in **11** are HOMO-11 and HOMO in Figure 3). The overall structure is the outcome of all bonding and antibonding combinations, but, since HOMO and HOMO-13 in **12** (or HOMO and HOMO-11 in **11**) counteract each other, the decisive π interactions in terms of vinylidene ligand orientation are those between the HOMO of the metal fragment and the LUMO of the C=CH_2 ligand.

Having varied the metal between **11** and **12**, we now investigate $[\text{Mo(C=C=CMePh)(dppe)}(\eta\text{-C}_7\text{H}_7)]^+$ (**10**), in which the cumulenylidene ligand is changed. The situation is somewhat more complicated, as there are now two π systems in C=C=CMePh and the lack of symmetry allows considerable hybridization of the orbitals on both fragments so that many fragment orbitals contribute a small but significant weight to the final molecular orbitals; Figure 5 shows the relevant orbitals. Applying the previous notion of the metal fragment HOMO and the cumulenylidene LUMO as the key interaction, we can quickly conclude that **10** should have the C=C=CR_2 unit oriented in a fashion opposite to that in **11**. HOMO-1 and HOMO-9 contain these interactions, and while these are clear in the latter, in HOMO-1 there is much hybridization, which makes the orbital quite difficult to look at. From the orbital analysis we find that, of the C=C=C(Me)Ph fragment orbitals that make up HOMO-1, some 14% comes from the LUMO of C=C=C(Me)Ph and 16% from the HOMO of the metal-containing fragment. We can "clean up" the orbitals by applying a localizing transformation to all the occupied orbitals and then order these orbitals by the diagonal elements of the Kohn–Sham matrix in the localized basis. Doing this, we find only one metal−cumulenylidene bonding orbital, which is directionally discriminate, for each system; these orbitals are shown in Figure 6.

Finally, if we consider the situation for the Mo system, for example, with the adducts next in the $(\text{C})_n\text{=CR}_2$ series, we expect that the orientation of the $(\text{C})_n\text{=CR}_2$ unit will be determined by the nature of its LUMO. Hence, for $n = 3$ the preferred orientation should be parallel with the Mo−Ct vector and for $n = 4$ it will be perpendicular, and so on. We also consider the oxacarbene ligand, $\overline{\text{CCH}_2\text{CH}_2\text{CH}_2\text{O}}$, whose complexation with Mo and Ru has been studied previously.[21,27] Figure 7 shows the LUMO orbitals for these ligands, and it is immediately apparent that the calculated orientation follows experimental observations. Thus, we find that for odd numbers of carbon centers the favored orientation has the $=\text{CR}_2$ plane

---

(57) Pipek, J.; Mezey, P. G. *J. Chem. Phys.* **1989**, *90*, 4916.

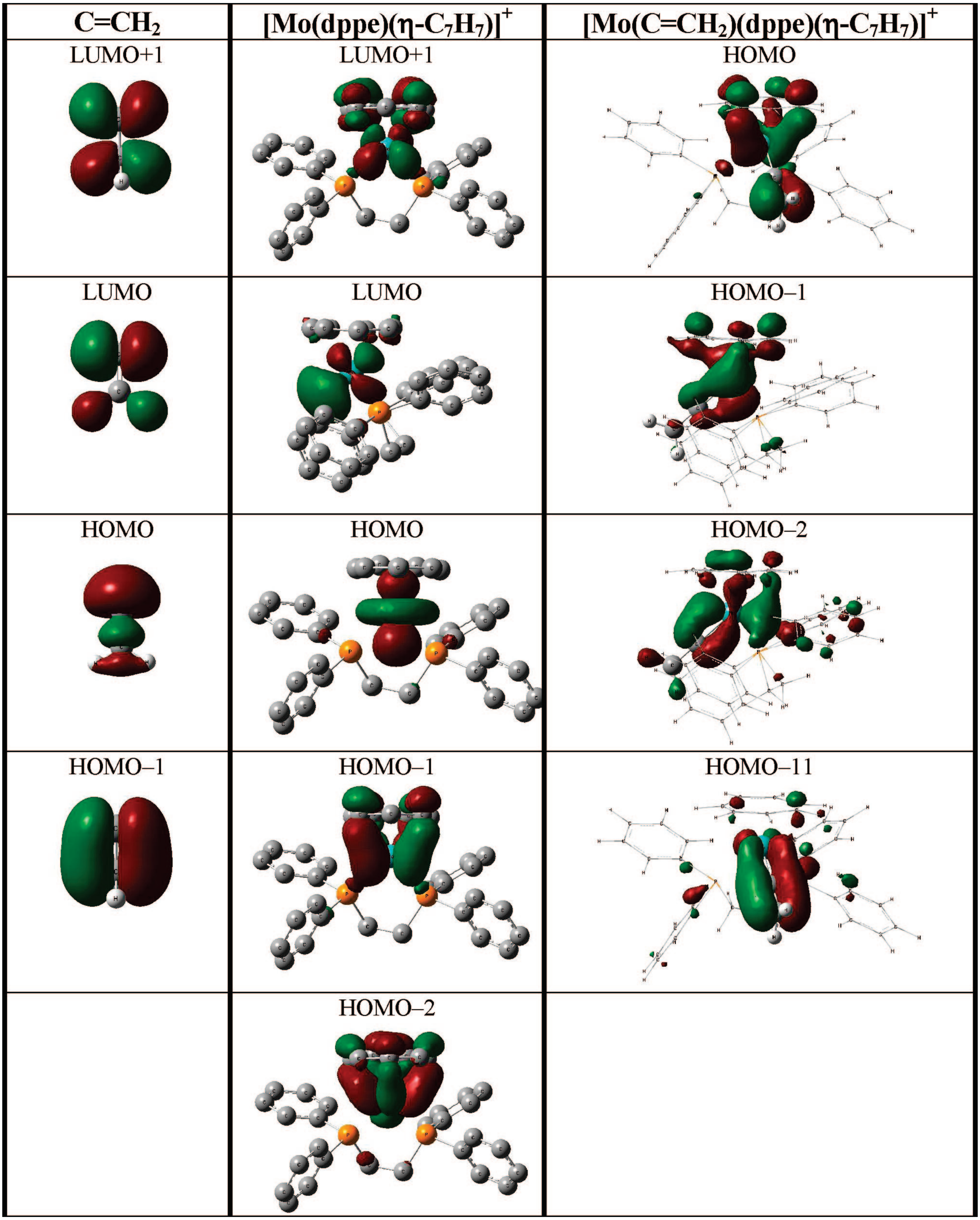

Figure 3. Key orbitals of C=CH$_2$, [Mo(dppe)(η-C$_7$H$_7$)]$^+$ (hydrogens omitted), and [Mo(C=CH$_2$)(dppe)(η-C$_7$H$_7$)]$^+$, plotted as isosurfaces of 0.04 au.

parallel to the plane of the C$_7$H$_7$ ring, while even numbers of carbon centers prefer the =CR$_2$ plane perpendicular.

Conclusions

The cycloheptatrienyl molybdenum system MoL$_2$(η-C$_7$H$_7$) (L$_2$ = P-donor ligand), with a formally d^6 metal center, promotes the isomerization of a wide range of terminal alkynes to afford a series of oxacyclocarbene, vinylidene, and allenylidene complexes of the general formulation [Mo{(C)$_n$=CR$_2$}L$_2$(η-C$_7$H$_7$)]$^+$ (n = 0−2; L$_2$ = P-donor ligand). X-ray structural studies from this and previous work reveal that the Mo(dppe)(η-C$_7$H$_7$) auxiliary controls the orientation of the cumulenylidene ligand

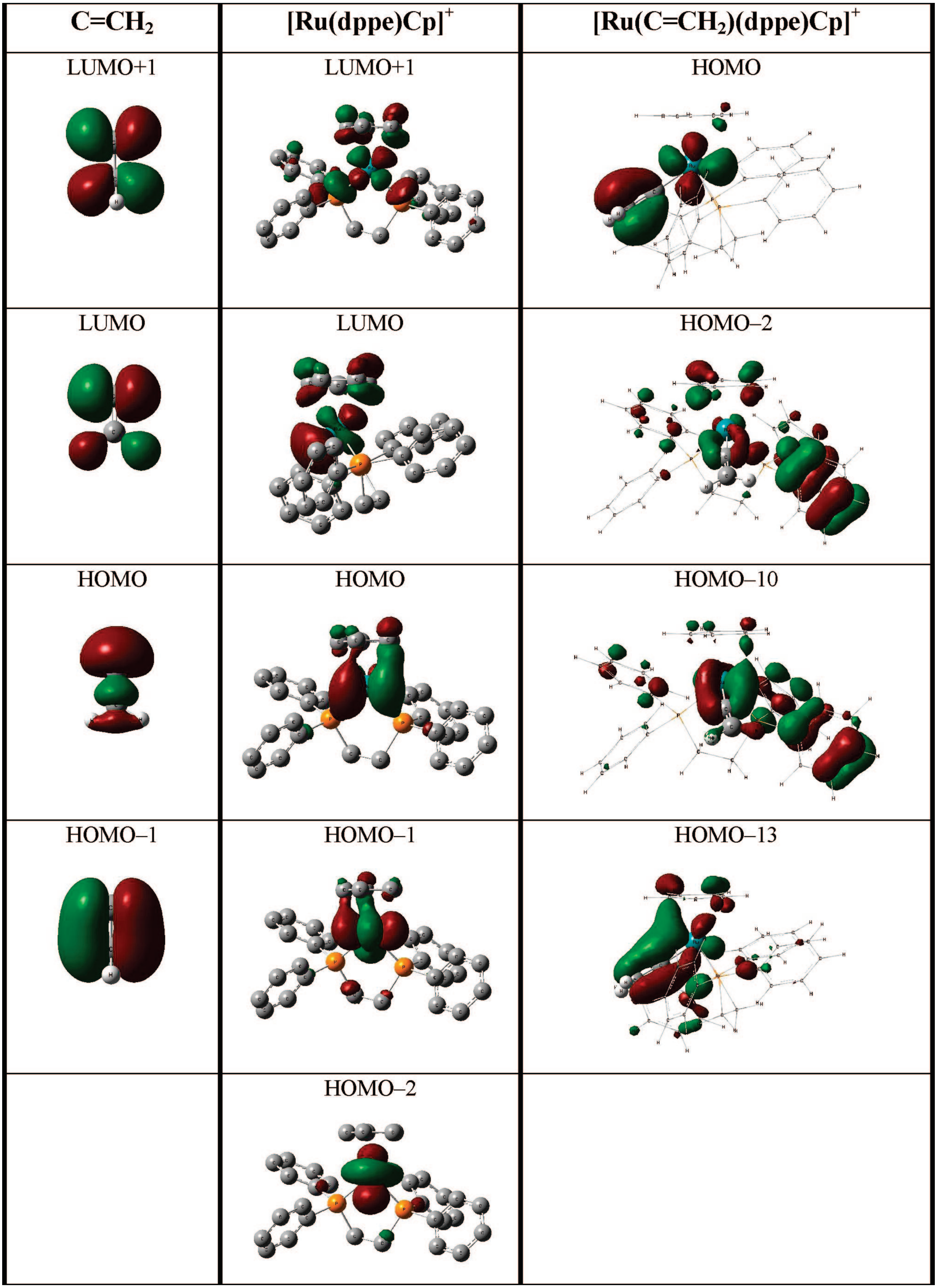

Figure 4. Key orbitals of $C{=}CH_2$, $[Ru(dppe)Cp]^+$ (hydrogens omitted), and $[Ru(C{=}CH_2)(dppe)Cp]^+$, plotted as isosurfaces of 0.04 au.

substituents to be the converse of the widely explored group 8 auxiliaries M(dppe)Cp (M = Fe, Ru). Thus, in complexes of the Mo(dppe)(η-C_7H_7) system, vinylidene ligands, $C{=}CR_2$, adopt a vertical arrangement in which the ligand R substituents lie in the

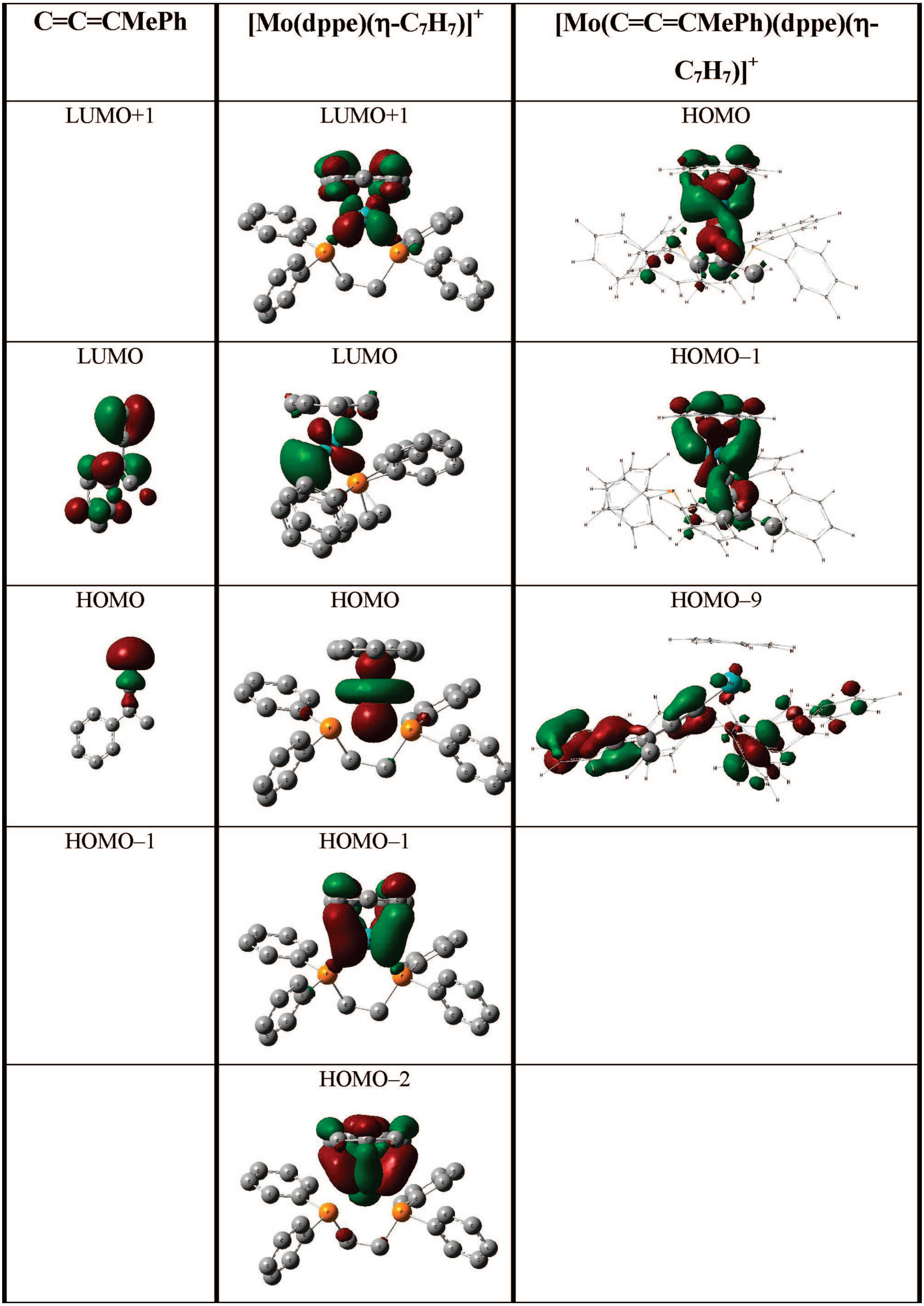

Figure 5. Key orbitals of C═C═CMePh, [Mo(dppe)(η-C_7H_7)]$^+$ (hydrogens omitted), and [Mo(C═C═CMePh)(dppe)(η-C_7H_7)]$^+$, shown as isosurfaces of 0.04 au.

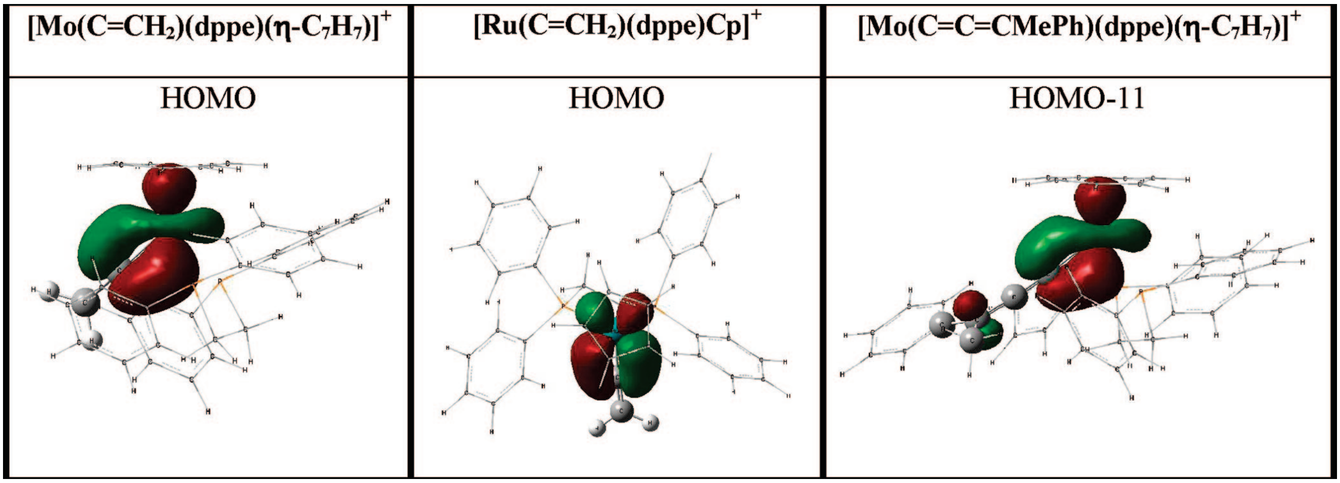

Figure 6. Localized orbitals of $[Mo(C{=}CH_2)(dppe)(\eta\text{-}C_7H_7)]^+$, $[Ru(C{=}CH_2)(dppe)Cp]^+$, and $[Mo(C{=}C{=}CMePh)(dppe)(\eta\text{-}C_7H_7)]^+$, plotted as isosurfaces of 0.04 au.

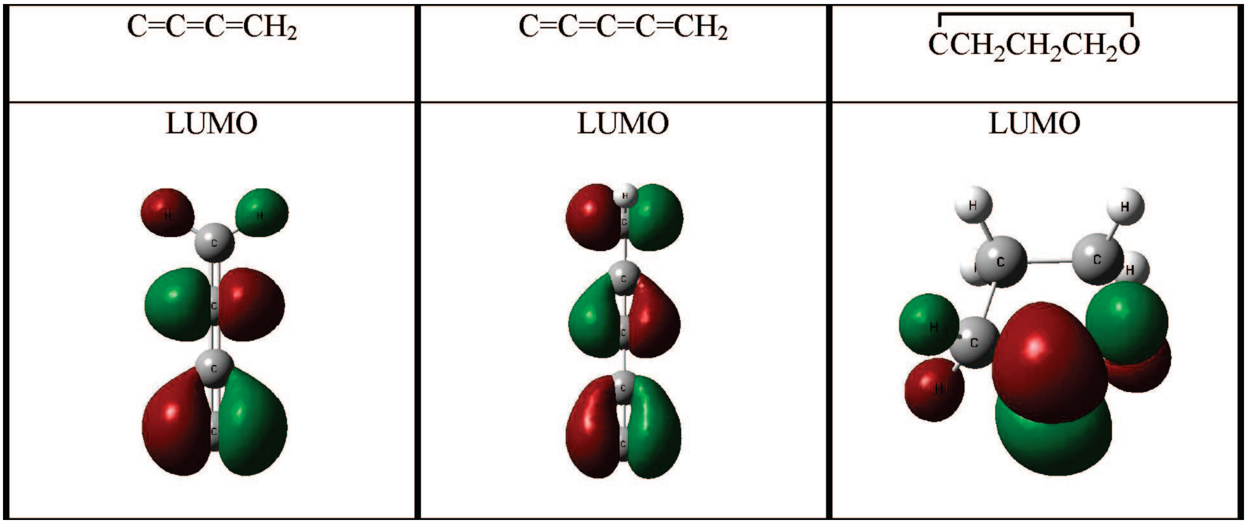

Figure 7. LUMO of $C{=}C{=}C{=}CH_2$, $C{=}C{=}C{=}C{=}CH_2$ and $\overline{CCH_2CH_2CH_2O}$ plotted as isosurfaces of 0.05 au.

pseudo mirror plane of the $Mo(dppe)(\eta\text{-}C_7H_7)$ fragment, whereas carbene and allenylidene ligands adopt a horizontal orientation with R substituents located orthogonal to the $Mo(dppe)(\eta\text{-}C_7H_7)$ mirror plane. As such, cumulenylidene complexes of the $Mo(dppe)(\eta\text{-}C_7H_7)$ auxiliary represent a unique example of a system in which these atypical ligand orientations are linked systematically by a proven, 90° rotation of the R substituents for each additional cumulenylidene ligand carbon. DFT calculations on the fragments $[Mo(dppe)(\eta\text{-}C_7H_7)]^+$ and $[Ru(dppe)Cp]^+$ reveal significant differences in the energy ordering of the respective MO manifolds. Critically the HOMO of the molybdenum system has substantial metal d_{z^2} character, whereas the HOMO of the $[Ru(dppe)Cp]^+$ fragment is based on a metal d_{xy} orbital, orthogonal to the HOMO of the $[Mo(dppe)(\eta\text{-}C_7H_7)]^+$ unit. In cumulenylidene complexes of the $Mo(dppe)(\eta\text{-}C_7H_7)$ auxiliary, interactions between the d_{z^2}-based HOMO of the metal fragment and the vacant LUMO of the cumulenylidene ligand dominate the control of ligand orientation. The importance of the d_{z^2}-based HOMO of the $Mo(dppe)(\eta\text{-}C_7H_7)$ fragment in metal−cumulenylidene bonding is manifested in the relatively large experimentally determined values (131–138°) for the angle $[Ct{-}Mo{-}C_\alpha]$, consistent with a tilting of the metal d_{z^2} orbital to maximize orbital overlap efficiency. The atypical ligand orientations imposed by the $Mo(dppe)(\eta\text{-}C_7H_7)$ auxiliary are further evident from dynamic NMR investigations. Low-temperature ^1H and $^{31}P\{^1H\}$ NMR spectra on the vertically orientated vinylidene complexes $[Mo\{C{=}C(H)(CH_2)_xPh\}(dppe)(\eta\text{-}C_7H_7)]^+$ reveal diasteroeomeric mixtures resulting from the location of the $(CH_2)_xPh$ substituent syn or anti to the cycloheptatrienyl ring. Variable-temperature $^{31}P\{^1H\}$NMR investigations on the horizontal, asymmetric allenylidene complex $[Mo(C{=}C{=}CMePh)(dppe)(\eta\text{-}C_7H_7)]^+$ (**10**) allowed estimation of the barrier to allenylidene ligand rotation as 57.8 kJ mol^{-1} at a coalescence temperature of 290 K.

Experimental Section

General Procedures. The preparation, purification, and reactions of the complexes described were carried out under dry nitrogen. All solvents were dried by standard methods, distilled, and deoxygenated before use. The compounds $[Mo(\eta\text{-}C_6H_5Me)(\eta\text{-}C_7H_7)][PF_6]$, $[MoBr(CO)_2(\eta\text{-}C_7H_7)]$, and $[MoI\{P(OMe)_3\}_2(\eta\text{-}C_7H_7)]$ were prepared by published procedures.[37,58,59] NMR spectra were recorded on Varian Inova 300 (300 MHz (^1H), 75 MHz ($^{13}C\{^1H\}$), 121.5 MHz ($^{31}P\{^1H\}$)) and Varian Inova 400 (400 MHz (^1H), 100

---

(58) Bochmann, M.; Cooke, M.; Green, M.; Kirsch, H. P.; Stone, F. G. A.; Welch, A. J. *J. Chem. Soc., Chem. Commun.* **1976**, 381.

(59) Hoch, G.; Panter, R.; Ziegler, M. L. *Z. Naturforsch.* **1976**, *31B*, 294.

MHz (^{13}C{^{1}H})) spectrometers. Infrared spectra were obtained on a Perkin-Elmer FT RX1 spectrometer, and mass spectra were recorded using Kratos Concept 1S (FAB spectra) and Micromass Platform II (ES spectra) instruments. Microanalyses were carried out by the staff of the Microanalytical Service of the School of Chemistry, University of Manchester.

Preparation of [MoBr(dppe)(η-C_7H_7)]·$0.5CH_2Cl_2$. A green solution of [MoBr(CO)$_2$(η-C_7H_7)] (3.50 g, 10.84 mmol) in toluene (120 cm^3) was warmed to 80 °C, and then dppe (2.156 g, 5.42 mmol) was added and the solution brought rapidly to reflux. After 1 h the resulting brown-green solution was treated with additional dppe (2.156 g, 5.42 mmol) and reflux continued for 18 h. The resulting olive green reaction mixture was filtered hot to remove a pink-red precipitate of [Mo(CO)(dppe)(η-C_7H_7)]Br (2.58 g) and then evaporated to dryness. The residue, dissolved in CH_2Cl_2, was transferred to an alumina/*n*-hexane chromatography column, and the product eluted as a green band using a *n*-hexane/CH_2Cl_2/acetone (1:1:1) solvent mixture as eluant. The green band was collected, solvent removed, and the residue recrystallized from CH_2Cl_2/*n*-hexane to give [MoBr(dppe)(η-C_7H_7)]·$0.5CH_2Cl_2$ as an olive green solid, yield 2.61 g (34%). Anal. Calcd for [MoBr(dppe)(η-C_7H_7)]·$0.5CH_2Cl_2$: C, 56.8; H, 4.5; Br, 11.3; Cl, 5.0. Found: C, 56.4; H, 4.5; (Br + Cl), 16.0.

Preparation of [Mo{$\overline{\text{CCH}_2\text{CH}_2\text{CH}_2\text{O}}$}(dppe)($\eta$-$C_7H_7$)][$PF_6$] (2). Method A. A green solution of [Mo(η-C_6H_5Me)(η-C_7H_7)][PF_6] (1.46 g, 3.44 mmol) in AR acetone (130 cm^3) was refluxed for 20 min and the resulting red solution treated with dppe (1.37 g, 3.44 mmol), after which time reflux was continued for 18 h. The green reaction mixture was then treated with 3-butyn-1-ol (0.80 g, 11.43 mmol) followed by further reflux for 3 h to give an orange solution, which was evaporated to dryness. Recrystallization of the residue from CH_2Cl_2/diethyl ether and then acetone/diethyl ether gave **2** as an orange solid; yield 2.01 g (73%). Anal. Calcd for $C_{37}H_{37}MoOP_3F_6$: C, 55.5; H, 4.6. Found: C, 55.6; H, 4.9. Mass (FAB): *m/z* 657 (M$^+$), 587 (M$^+$ − C_4H_6O). The complexes [Mo{$\overline{\text{CCH}_2\text{CH}_2\text{CH}_2\text{O}}$}(dppm)($\eta$-$C_7H_7$)][$PF_6$] (**1**) and [Mo{$\overline{\text{CCH}_2\text{CH}_2\text{CH}_2\text{CH}_2\text{O}}$}(dppm)($\eta$-$C_7H_7$)][$PF_6$] (**3**) were prepared by an analogous procedure. Complex **1** was obtained in 54% yield starting from [Mo(η-C_6H_5Me)(η-C_7H_7)][PF_6] (0.44 g, 1.04 mmol), dppm (0.40 g, 1.04 mmol), and 3-butyn-1-ol (0.35 g, 5.00 mmol). Anal. Calcd for $C_{36}H_{35}MoOP_3F_6$: C, 55.0; H, 4.5. Found: C, 54.5; H, 4.9. Mass (FAB): *m/z* 644 (M$^+$ + 1), 573 (M$^+$ − C_4H_6O). Complex **3** was prepared in 9% yield from [Mo(η-C_6H_5Me)(η-C_7H_7)][PF_6] (1.01 g, 2.38 mmol), dppm (0.91 g, 2.38 mmol), and 4-pentyn-1-ol (0.40 g, 4.76 mmol). Anal. Calcd for $C_{37}H_{37}MoOP_3F_6$: C, 55.5; H, 4.6. Found: C, 55.8; H, 4.8. Mass (FAB): *m/z* 657 (M$^+$), 573 (M$^+$ − C_5H_8O).

Method B. A mixture of [MoBr(dppe)(η-C_7H_7)]·$0.5CH_2Cl_2$ (0.50 g, 0.71 mmol), 3-butyn-1-ol (0.26 g, 3.71 mmol), and K[PF_6] (0.28 g, 1.52 mmol) in AR methanol (40 cm^3) was refluxed for 1.5 h, and the resulting orange-red solution was evaporated to dryness. Recrystallization of the residue from CH_2Cl_2/diethyl ether and then acetone/diethyl ether gave **2** as an orange solid; yield 0.49 g (86%).

Preparation of [Mo{$\overline{\text{CCH}_2(\text{CH}_2)_2\text{CH}_2\text{O}}$}(dppe)($\eta$-$C_7H_7$)][$PF_6$] (4). Method A. A mixture of [MoBr(dppe)(η-C_7H_7)]·$0.5CH_2Cl_2$ (0.50 g, 0.71 mmol), 4-pentyn-1-ol (0.32 g, 3.80 mmol), and K[PF_6] (0.28 g, 1.52 mmol) in AR methanol (40 cm^3) was refluxed for 72 h, and the resulting orange-red solution was evaporated to dryness. The residue was dissolved in CH_2Cl_2 and the solution filtered, reduced in volume to 10 cm^3, and then treated with diethyl ether (30 cm^3) to precipitate the crude product as a yellow-orange solid. Recrystallization from acetone/diethyl ether gave **4** as a yellow-orange solid; yield 0.29 g (50%). Anal. Calcd for $C_{38}H_{39}MoOP_3F_6$: C, 56.0; H, 4.8. Found: C, 55.9; H, 5.2. Mass (FAB): *m/z* 671 (M$^+$), 587 (M$^+$ − C_5H_8O).

Method B. A mixture of [Mo{C=C(H)$CH_2CH_2CH_2OH$}(dppe)(η-C_7H_7)][PF_6] (**5**; 0.34 g, 0.42 mmol) and LiCl (0.02 g, 0.04 mmol) was refluxed in acetone (60 cm^3) for 18 h and the solvent then removed. The residue was dissolved in CH_2Cl_2 and the solution filtered and reduced in volume to 10 cm^3. Fractional crystallization by slow addition of diethyl ether gave complex **4** as a yellow solid as the second precipitated fraction; yield 0.06 g (18%).

Preparation of [Mo{C=C(H)$CH_2CH_2CH_2OH$}(dppe)(η-C_7H_7)][PF_6] (5). A green solution of [Mo(η-C_6H_5Me)(η-C_7H_7)][PF_6] (0.50 g, 1.18 mmol) in AR acetone was refluxed for 20 min and the resulting red solution treated with dppe (0.47 g, 1.18 mmol), after which time reflux was continued for 18 h. The green reaction mixture was then treated with 4-pentyn-1-ol (0.20 g, 2.38 mmol) followed by further reflux for 30 min to give an orange solution, which was evaporated to dryness. Recrystallization of the residue from methanol/diethyl ether and then acetone/diethyl ether gave **5** as an orange solid; yield 0.30 g (31%). Anal. Calcd for $C_{38}H_{39}MoOP_3F_6$: C, 56.0; H, 4.8. Found: C, 56.3; H, 5.0. Mass (FAB): *m/z* 670 (M$^+$ − H), 587 (M$^+$ − C_5H_8O).

Preparation of [Mo{C=C(H)CH_2CH_2Ph}(dppe)(η-C_7H_7)][PF_6] (6). A green solution of [Mo(η-C_6H_5Me)(η-C_7H_7)][PF_6] (0.50 g, 1.18 mmol) in AR acetone was refluxed for 20 min and the resulting red solution treated with dppe (0.47 g, 1.18 mmol), after which time reflux was continued for 18 h. The green reaction mixture was then treated with 4-phenyl-1-butyne (0.31 g, 2.38 mmol) followed by further reflux for 3 h to give an orange solution, which was evaporated to dryness. Recrystallization of the residue from CH_2Cl_2/diethyl ether and then acetone/diethyl ether gave **6** as an orange solid; yield 0.62 g (61%). Anal. Calcd for $C_{43}H_{41}MoP_3F_6$: C, 60.0; H, 4.8. Found: C, 59.8; H, 4.7. Mass (FAB): *m/z* 717 (M$^+$), 587 (M$^+$ − $C_{10}H_{10}$). Orange [Mo{C=C(H)CH_2Ph}(dppe)(η-C_7H_7)][PF_6] (**7**) was obtained by an analogous procedure in 18% yield starting from [Mo(η-C_6H_5Me)(η-C_7H_7)][PF_6] (0.50 g, 1.18 mmol), dppe (0.47 g, 1.18 mmol), and 3-phenyl-1-propyne (0.27 g, 2.33 mmol), except that recrystallization of the crude product was from methanol/diethyl ether followed by acetone/diethyl ether. Anal. Calcd for $C_{42}H_{39}MoP_3F_6$: C, 59.6; H, 4.6. Found: C, 59.7; H, 4.6. Mass (FAB): *m/z* 703 (M$^+$), 587 (M$^+$ − C_9H_8).

Preparation of [Mo{C=C(H)Ph}{P(OMe)$_3$}$_2$(η-C_7H_7)][BF_4] (8). A mixture of [MoI{P(OMe)$_3$}$_2$(η-C_7H_7)] (1.89 g, 3.36 mmol), HC≡CPh (5.14 g, 50.39 mmol), and K[PF_6] (0.93 g, 5.05 mmol) in methanol (40 cm^3) was stirred at 20 °C for 3 h, resulting in a color change from green to orange. The reaction solution was evaporated to dryness and the residue, dissolved in AR acetone (60 cm^3), was treated with KOBu^t (0.75 g, 6.70 mmol) and stirred for 1 h to give a red-brown solution, from which the solvent was removed. The resulting solid, dissolved in CH_2Cl_2, was transferred to a *n*-hexane/alumina chromatography column, and elution with *n*-hexane/acetone (2:1) gave a purple band, which was collected and solvent removed to give crude [Mo(C≡CPh){P(OMe)$_3$}$_2$(η-C_7H_7)] as a purple oil. The intermediate alkynyl complex was dissolved in diethyl ether (50 cm^3) cooled to −78 °C and H[BF_4] (54 wt% in diethyl ether) (0.23 g, 2.61 mmol) added to the stirred solution. When the mixture was warmed to room temperature, an oily orange precipitate formed, which was dried in vacuo and then washed with diethyl ether (2 × 10 cm^3), methanol (1 × 2 cm^3), and finally diethyl ether (1 × 10 cm^3) to give **8** as an orange solid; yield 1.17 g (56%). Anal. Calcd for $C_{21}H_{31}MoO_6P_2BF_4$·CH_3OH: C, 40.2; H, 5.3. Found: C, 39.6; H, 5.1. Mass (ES in NCMe): *m/z* 539 (M$^+$), 415 (M$^+$ − P(OMe)$_3$).

Preparation of [Mo(C=C=CPh_2)(dppe)(η-C_7H_7)][PF_6] (9). A mixture of [MoBr(dppe)(η-C_7H_7)]·$0.5CH_2Cl_2$ (0.75 g, 1.06 mmol), HC≡CCPh_2(OH) (0.47 g, 2.26 mmol), and K[PF_6] (0.42 g, 2.28 mmol) in methanol (40 cm^3) was refluxed for 12 h to give a purple-brown solution, which was evaporated to dryness. The residue was dissolved in CH_2Cl_2 and transferred to a *n*-hexane/alumina chromatography column. Elution with a *n*-hexane/acetone mixture (10:1 increasing to 1:1) resulted in elution of a yellow band, closely followed by a deep purple band. The deep purple band was collected and evaporated to dryness and the crude product recrystallized from acetone/diethyl ether to give **9** as a deep purple solid; yield 0.20 g (21%). Anal. Calcd for $C_{48}H_{41}MoP_3F_6$: C, 62.6; H, 4.5. Found: C, 62.6; H, 4.6. Mass (FAB): *m/z* 777 (M^+), 587 ($M^+ - C_3Ph_2$). IR ν(C=C=C) (CH_2Cl_2): 1876 cm^{-1}.

Preparation of [Mo(C=C=CMePh)(dppe)(*η*-C_7H_7)][PF_6] (10). A mixture of [MoBr(dppe)(η-C_7H_7)]·0.5CH_2Cl_2 (1.50 g, 2.12 mmol), HC≡CCMePh(OH) (0.83 g, 5.68 mmol), and K[PF_6] (0.65 g, 3.53 mmol) in methanol (100 cm^3) was refluxed for 2 h to give a purple solution, which was evaporated to dryness. The residue was dissolved in CH_2Cl_2 and transferred to a *n*-hexane/silica chromatography column. Elution with *n*-hexane/CH_2Cl_2 (1:1) followed by CH_2Cl_2/acetone (20:1) resulted in elution of a yellow band, closely followed by a deep purple band. The deep purple band was collected and evaporated to dryness and the crude product recrystallized from acetone/diethyl ether to give **10** as a deep purple solid; yield 0.17 g (9%). Anal. Calcd for $C_{43}H_{39}MoP_3F_6$: C, 60.1; H, 4.5. Found: C, 59.5; H, 4.6. Mass (FAB): *m/z* 715 (M^+), 587 ($M^+ - C_3MePh$). IR ν(C=C=C) (CH_2Cl_2): 1876 cm^{-1}.

X-ray Crystal Structures of [Mo{C=C(H)Ph}{P(OMe)$_3$}$_2$(*η*-C_7H_7)][BF_4]·MeOH (8) and [Mo(C=C=CPh$_2$)(dppe)(*η*-C_7H_7)]-[PF_6]·0.25CH_2Cl_2 (9). The majority of details of the structure analyses carried out on complexes **8** and **9** are given in Table 6. Single crystals of **8** were obtained as red plates by recrystallization from methanol at −20 °C, and a crystal of dimensions 0.30 × 0.30 × 0.10 mm was selected for analysis. Single crystals of **9** were obtained as deep purple plates by vapor diffusion of diethyl ether into a CH_2Cl_2 solution of the complex, and a crystal of dimensions 0.35 × 0.35 × 0.10 mm was used for analysis. Data collection, cell refinement, and data reduction were carried out with Bruker SMART and Bruker SAINT software; SHELXS-97[60] (**8**) or SIR-97[61] (**9**) was employed for the computing structure solution and SHELXL-97[62] for the computing structure refinement. In each case an absorption correction was applied with the aid of the SADABS program.[63] Both structures were solved by direct methods with refinement by full-matrix least squares based on F^2. The asymmetric units of **8** and **9** contain solvent of crystallization; in the case of complex **9** the CH_2Cl_2 is disordered with a 0.25 occupancy. All non-hydrogen atoms were refined anisotropically, with the exception of the disordered CH_2Cl_2 of **9**; in complex **9**, hydrogen atoms were included in calculated positions, but in **8** the H atoms were located by difference Fourier techniques and refined isotropically.

Table 6. Crystal Data and Refinement Parameters for [Mo{C=C(H)Ph}{P(OMe)$_3$}$_2$(*η*-C_7H_7)][BF_4]·MeOH (8) and [Mo(C=C=CPh$_2$)(dppe)(*η*-C_7H_7)][PF_6]·0.25CH_2Cl_2 (9)

	8	9
formula	$MoC_{22}H_{35}P_2O_7BF_4$	$MoC_{48.25}H_{41.5}P_3Cl_{0.5}F_6$
mass (amu)	656.19	941.89
temp (K)	100(2)	100(2)
λ (Å)	0.710 73 (Mo Kα)	0.710 73 (Mo Kα)
cryst syst	monoclinic	monoclinic
space group	$P2_1/n$	$P2_1/c$
a (Å)	10.5384(14)	11.5260(8)
b (Å)	13.0298(17)	17.7669(13)
c (Å)	20.266(3)	20.4687(15)
β (deg)	93.439(2)	99.6210(10)
V (Å^3); *Z*	2777.8(6); 4	4132.7(5); 4
abs coeff (cm^{-1})	6.53	5.28
θ range (deg)	1.86–26.46	1.79–26.38
limiting indices (*h*, *k*, *l*)	−13 to +12, ±16, −25 to +16	−11 to +14, ±22, −24 to +25
total no. of rflns	15 368	23 732
no. of indep rflns, $I > 2\sigma(I)$	5686	8425
R1	0.0343	0.0483
wR2	0.0730	0.1247
completeness to θ (%)	99.3	99.5

Acknowledgment. We thank the EPSRC for research studentships (to R.W.G. and Z.I.H.) and for support of the computational work through Grant No. EP/E025544/1.

Supporting Information Available: CIF files giving X-ray crystallographic data for complexes **8** and **9**. This material is available free of charge via the Internet at http://pubs.acs.org.

OM700920T

---

(60) Sheldrick, G. M. *SHELXS-97, Program for Crystal Structure Solution*; Universität Göttingen, Göttingen, Germany, 1997.

(61) Altomare, A.; Burla, M. C.; Camalli, M.; Cascarano, G. L.; Giacovazzo, C.; Guagliardi, A.; Moliterni, A. G. G.; Polidori, G.; Spagna, R. *J. Appl. Crystallogr.* **1999**, *32*, 115.

(62) Sheldrick, G. M. *SHELXL-97, Program for Crystal Structure Refinement*; Universität Göttingen, Göttingen, Germany, 1997.

(63) Sheldrick, G. M. *SADABS, an Empirical Absorption Corrections Program*; Universität Göttingen, Göttingen, Germany, 1997.